ENCLOSURE 2

MFN 14-064

Response to Request for Additional Information Re: GEH Licensing Topical Report NEDE-33005P, Revision 0, "TRACG Application for Emergency Core Cooling Systems / Loss-of-Coolant-Accident Analyses for BWR/2-6"

Non-Proprietary Information – Class I (Public)

IMPORTANT NOTICE

This is a non-proprietary version of Enclosure 1, from which the proprietary information has been removed. Portions of the enclosure that have been removed are indicated by an open and closed bracket as shown here [[ ]].

Note to the Reviewers

In a number of requests for additional information (RAI), there is a common concern regarding the magnitude of the non-phenomenological uncertainty, or the variability (noise) of the results. This noise is a result of an exaggerated sensitivity to a bifurcation in the channel flow responses (parallel channel effect, plugging/unplugging). In particular, RAIs 4 through 10 express concerns related to this noise. In response to these concerns, GE Hitachi Nuclear Energy (GEH) improved the core modelling detail (RAIs 6 and 9) to minimize the exaggerated sensitivity to the bifurcation in the channel flow responses. Consequently, to a large extent the reduced noise has mitigated the Nuclear Regulatory Commission (NRC) concerns. GEH commits to use detailed core modeling in the application of the methodology to plant licensing calculations.

GEH is planning to update the LTR to issue a Revision 1 to include the changes discussed in the "LTR Impact" sections of the RAI response along with additional editorial corrections. This revision is expected to be submitted as part of RAI response closure, before the SER is issued on the methodology.

RAI-1

1) The NRC staff requests additional technical basis to justify the adequacy of statistical distributions presented in section 5.1 of the topical report (TR) that are used to determine 95/95 upper tolerance limits for comparison to the criteria of Title 10 of the *Code of Federal Regulations*(10 CFR) Part 50.46. Please address the following issues either generically and/or for specific phenomena and parameters, as necessary:

   a. Due to the strong influence of the data selection process on the resulting statistical distributions, objective rationale should be provided for the selection of test data and, equivalently, the implicit rejection of other potentially applicable data. Although some datasets may be more relevant than others, excessive selectivity could lead to underestimation of the true uncertainty.

   b. Some data populations used in the TR are of limited size, and it is not apparent whether sufficient statistical power exists to justify conclusions regarding normality and other distribution characteristics. Although the probability for Type I error is established by the confidence level, the probability for Type II error can grow quite large as the sample size is reduced.

   c. Please provide additional technical basis to justify the adequacy of statistical uncertainty distributions that are dependent on the data used to develop closure relations in the code (e.g., phenomenon identification and ranking table (PIRT) items A1, C26, F3, etc.). In this case, how does GEH account for the fact that the statistical distribution does not include a bias and/or fully account for the standard deviation that realistically may exist (e.g., due to issues such as those discussed in parts d. and e. below).

   d. Due to the potential for systematic error, the statement in section 5.0 of the TR that measurement error is implicitly included in comparisons of code predictions with test data appears correct based on the NRC staff's understanding only when data from multiple test programs is considered. In light of the discussion above, please clarify GEH's position on how systematic error is accounted for if data from diverse sources is not used in deriving uncertainty distributions.

   e. To avoid underestimating the true uncertainty, what consideration did GEH give to the fact that test conditions are generally idealized, simplified, and well controlled relative to complex plant conditions under which derived correlations and models are applied? For example, simplified geometries and reduced scales may lead to underestimation of uncertainty, steady state uncertainty may be less than transient uncertainty, and the uncertainty may increase in an extrapolated transition region between the validation ranges of two correlations.

RAI-1 Response

   a. To the extent possible and practical, rationale for selection of certain test data and rejection of other data for determining the model uncertainties are explained in the LTR. Resulting model uncertainty depends on the underlying data; however, the selection

process is neutral and independent from final distributions. In general, principles like applicability, geometry similarities, as well as the data availability and reliability, are used.

b. Although some data populations used in the development of uncertainty distributions are of limited size, use of limited dataset ultimately penalizes the methodology by imposing a relatively larger uncertainty. Regarding the Type II errors, knowing the exact shape of the probability distribution for a given uncertainty parameter is less important than whether the statistics (bias and standard deviation with an associated distribution) applied for that parameter adequately covers the observed model uncertainties, for the application methodology. Increasing the population size for the underlying data used in model uncertainty evaluation could ultimately reduce the overall phenomenological uncertainties; but, having a limited population does not per se invalidate the systematic approach that was employed in development of the probability density functions. The essential need being addressed by the methodology is that the modeled uncertainty distribution represents either realistically or conservatively the tail of the distribution that will contribute to the tolerance limit of the critical licensing parameters associated with PCT and oxidation.

c. In the U.S., all the current state-of-the-art best-estimate methodologies are similar in this aspect: they all rely on, to a certain extent, the same data to determine the code bias and uncertainties as well as to qualify specific aspects of the models. This, however, is not a deficiency since the model formulations themselves are to the greatest extent possible based on physical models and/or scalable dimensionless parameters rather than a brute-force correlation of the raw data. One should expect that any purely empirical fit to a complete dataset would represent that dataset without any bias and should be applied cautiously or nor at all outside the range spanned by the data. The GEH approach is whenever possible to select separate effect tests that isolate the phenomenon of interest and use data from these tests to quantify the uncertainty and bias associated with the modeling of that phenomenon. The approach is checked by applying all the relevant biases and uncertainties to the simulation of integral system tests and plant cases (where multiple phenomena are interacting) to confirm that coverage of the experimental data variability is achieved. The types of data for the integral tests and plant cases tend to be macroscopic quantities such as clad temperatures, pressures, flows, etc. that depend on many separate modeling phenomena in much the same way as the critical licensing parameters.

d. The statement in Section 5.0 indicates that the measurement uncertainty in the data is intrinsically accounted for when code comparison to experimental results is made. No further attempt to minimize or eliminate any potential systematic error in the experimental data is being made. If a systematic error exists in the experimental data, and if, without consideration of data from multiple test programs, it propagates through the evaluation, it will ultimately add more uncertainty. By using bias and uncertainty with potential systematic error, the methodology could lack a further refinement, but will

still capture at a minimum the uncertainty associated with the phenomena. From the methodology development point of view, that kind of compromise is deemed acceptable by GEH.

e. Whenever possible, the uncertainty for each phenomenon must be obtained from separate effects tests, not from integral effects tests, as explained in part (c) of the response. The GEH approach is consistent with this principle. How the biases and uncertainties from separate phenomena combine into composite biases and uncertainties of macroscopic quantities depends on the interactions of the phenomena and their relative importance to the macroscopic parameter. These relative importances change depending on the facility being modeled, the modeling scenario, and even change with time during the scenario. It is the interactions within the code simulation that determine how a certain bias and uncertainty for a specific phenomenon will be manifested in the output parameter. The main reason GEH has applied the TRACG LOCA methodology to integral tests as documented in Section 7 of the LTR is to illustrate how separate biases and uncertainties via complex interactions among competing processes manifest themselves as uncertainties and biases in the macroscopic output parameters. The statistical results from the transient integral test simulations compared to macroscopic data from these tests supports the conclusion that the predicted biases and uncertainties of the macroscopic parameters are not underestimated.

LTR Impact

No changes to the LTR are proposed as the result of this RAI response.

RAI-2

2) The NRC staff requests additional technical basis to justify the adequacy of neglecting statistical dependencies between random variable input parameters. The TR generally appears to treat statistical parameters independently, although some parameters would presumably be correlated. Neglect of statistical correlation between input parameters could lead to underestimation of 95/95 upper tolerance limits. Therefore, please describe the approach for identifying and accounting for statistical dependencies between input parameters and justify its adequacy, with emphasis on the issues below.

   a. In a number of cases, random variables used to generate uncertainty for a model or correlation that is used in multiple locations within the computational domain are assumed to be independent. Although part of the uncertainty associated with a correlation may be attributable to uncorrelated differences in local parameters (e.g., flow conditions), generally, GEH's technical basis for presuming that there is no linkage between predictions from the same model in different spatial components could not be discerned from the NRC staff's review of the TR, especially where similar flow regimes exist. The following examples (not all-inclusive) illustrate the issue:

      i. The Lee-Ryley correlation is used to calculate interfacial heat transfer within a variety of spatial components in the computational model, with independent, identically distributed random variable multipliers selected to perturb the heat transfer in each component. However, a significant piece of the model uncertainty is presumably driven by limitations residing in the Lee-Ryley correlation itself (e.g., the assumption of spherical bubbles), which would seemingly distort predictions in multiple spatial locations similarly.

      ii. Similar conclusions apply to statistical distributions for other models used in multiple regions of the computational domain, such as those for interfacial drag, interfacial shear and entrainment, heat transfer (Chen, Dittus-Boelter), etc.

      iii. Internal rod pressures may be correlated within a given assembly or section of core with a higher peaking than predicted.

      iv. The thickness of an oxide or crud layer on fuel rods may depend on conditions common to all rods, and may affect all correlations for heat transfer from the fuel.

   b. Uncertainties associated with predicting some parameters, for example interfacial heat transfer and interfacial drag / shear, are presumably correlated with each other through one or more fundamental input random variables influencing both parameters (e.g., in this case, interfacial area concentration and relative phase velocity). Please clarify how independence is assured in the selection of random parameters, or explain how the potential for correlation between random parameters is accounted for in the methodology.

RAI-2 Response

From a statistical point of view, if two or more parameters are statistically correlated, assuming independent uncertainty distributions would not lead to underestimation of upper tolerance limits of the output parameters. This can be visualized, in simple terms, by an example of combining two distributions with different mean values. The combined distribution would have lower frequency for the mean value, but a larger spread, i.e. uncertainty. This, in turn, would yield a higher upper tolerance limit for the uncertainty contributor. In other words, chances of sampling more extreme values of the input in the statistical analysis. In the practical applications, however, if the parametric effects are counterbalanced, or in other words, they have cancelling effect, the concern as explained in the RAI cannot be ignored.

The TRACG LOCA methodology considers the dependencies of the model uncertainties, in the statistical sampling process. In the application process, there exist provisions for determining to be done either concurrently or independently. [[

]]

In summary, the TRACG LOCA methodology does not neglect the potential effects of dependencies between random variable input parameters. According to the physical phenomena they represent and consistent with observed or expected actual behavior from plant conditions, the uncertainty contributors are either sampled and applied concurrently or independently for different components in the input model, as explained above.

LTR Impact

No changes to the LTR are proposed as the result of this RAI response.

RAI-3

3) A number of nodalization variations presented in Table 5.2-1 of the TR result in predicted changes to the peak cladding temperature (PCT) for a BWR/4 that approach or exceed the significance threshold of 50°F in 10 CFR 50.46 for changes or errors to a methodology. Estimating the aggregate effect of nodalization variations based on the available data shows that the potential range of cumulative variation is large (i.e., sum of absolute values of ΔPCT values in Table 5.2-1), particularly for the potentially limiting intermediate break. Further, there appears to be potential for an increase in PCT that could be significant (e.g., sum of ΔPCT values in Table 5.2-1). As such, it is unclear that nodalization error is small relative to the uncertainties determined in the demonstration analysis in Chapter 8 of the TR or on par with time step variations of the magnitude shown in Figure 6.9-5 of NEDE-32177P, Revision 3. Therefore, please address the following requests:

   a. Either (1) reduce the uncertainty band associated with nodalization to a level that is small relative to other uncertainties that are explicitly accounted for by the methodology, (2) reasonably estimate the nodalization error and include an allowance for this error in the methodology (e.g., through the analysis resolution), or (3) adequately justify the current approach.

   b. Please provide results of similar nodalization and time step studies that are applicable to the expected limiting break for the BWR/2 design and further address the request in Part a. (above) considering the potential for limited margins to regulatory criteria.

RAI-3 Response

Summing the absolute value of the variations indicated by the nodalization studies is not the correct process for comparison to the significance threshold of 50°F in 10 CFR 50.46. The 10 CFR 50.46 criteria apply to changes in the model from the approved baseline. A standard nodalization has been proposed for purposes of establishing the baseline modeling to be approved and it is differences caused by deviations from this approved nodalization that will be subject to the 50°F threshold.

a. In response to other RAIs, RAI-6 and RAI-9 in particular, [[

]]

The first row in Table 5.2-1 provides baseline PCT values that are [[

]]

b. The nodalization and time step studies applicable to the BWR/2 design have been performed as sensitivities to the BWR/2 limiting break scenario [[

]] Table R3-1 summarizes the results from these nodalization sensitivity studies.

The analysis results presented in Table R3-1 demonstrate that in each of the sensitivity cases, the effect on the PCT is relatively small compared to the overall uncertainty of the statistical runs [[

]] The study results are summarized graphically in Figures R3-1 and R3-2. These results will also be incorporated into Section 5.2 of the LTR.

LTR Impact

The results of the BWR/2 nodalization sensitivity study will be incorporated into Section 5.2 of the LTR. Table R3-1 will be added to the LTR as Table 5.2-2, and the title of Table 5.2-1 will be revised to distinguish it from Table 5.2-2. Figures R3-1 and R3-2 will be added as Figures 5.2-10 and 5.2-11. This added information, like that previously presented for jet-pump BWRs in LTR Table 5.2-1, is [[

]] GEH has committed to perform all future plant evaluations and applications using the detailed core models.

Table R3-1 Summary of Nodalization Sensitivity Studies for BWR/2 Using the Original LTR Core Model

[[		
		]]

[[

]]

Figure R3-1 Vessel Axial Nodalization Sensitivity for BWR/2

[[

]]

Figure R3-2 Channel Axial Nodalization Sensitivity for BWR/2

RAI-4

4) In a number of places in the TR, the proposed disposition of certain evaluation model parameters (e.g., [[

]] (e.g., Table 5.2-1, section 8.1.3, section 8.1.4, Table 8.1-12, section 5.1.8.2). In light of the potential for random noise to cause significant variation in figures of merit in certain scenarios, please discuss to what extent single-simulation sensitivity studies genuinely reflect the expected influence of parameter perturbations in future statistical calculations for a similar reactor design, versus being attributable to random, noise-level perturbations. Please discuss measures taken to ensure that the results of sensitivity studies provide useful and representative data (e.g., sensitivity cases are performed with noise-driven phenomena such as the "parallel channel effect" held constant or from multiple simulations with varied noise-level inputs).

RAI-4 Response

[[

]] These results are presented as part of the response to RAI-6 and RAI-9. GEH believes that with this smaller variability that single-simulation sensitivity studies can now provide a reasonable means to screen potential effects. Single-simulation sensitivity studies are appropriate to support technical justification for particular applications provided the results are not contrary to experience and physical principles. If a decision is to be made based on the direction and/or magnitude of the conservatism which is not known, then averaging of additional cases to eliminate or reduce the impact of 'random noise' can be utilized to better quantify the conservatism. In summary, a small PCT analysis resolution, i.e. a small variability associated with non-phenomenological uncertainty, enhances the robustness of the methodology. The commitment to use the detailed core models for all plant applications is the main measure taken to ensure that future sensitivity studies will provide useful and representative results.

LTR Impact

No changes to the LTR are proposed as the result of this RAI response. GEH acknowledges that the nodalization sensitivity studies shown in the LTR Table 5.2-1 and new results produced for the BWR/2 in response to RAI-3 [[ ]]
GEH does not intend to update these studies in the LTR for the reasons indicated in the response to RAI-3.

RAI-5

5) The TR asserts in section 6.4 that the range of PCT results conservatively accounts for the "parallel channel effect" via either normal distribution statistics or order statistics. However, no evidence is presented that the parallel channel behavior predicted by the TRACG [GEH proprietary version of the Transient Reactor Analysis Code (TRAC)] evaluation model would accurately represent multi-channel behavior in a reactor core. For example, due in part to phenomenological uncertainties as well as the grouping of bundles in the TRACG evaluation model, it is not clear that the probability of the TRACG peak-PCT bundle not being "plugged" with liquid is equivalent to the probability of all bundles in a reactor core containing similarly hot rods being unplugged during a LOCA. Without evidence of equivalence in this and similar comparisons between the evaluation model and an actual reactor core, confidence cannot exist that the parallel channel effect is realistically accounted for through upper tolerance limits derived from either normal distribution statistics or order statistics. In light of the discussion above, please address the following points:

   a. Either revise the TRACG evaluation model to account for the uncertainties associated with the parallel channel effect conservatively or (if justifiable) realistically, or provide sufficient evidence to justify that the parallel channel effect is simulated by the existing TRACG evaluation model in a physically and statistically representative manner.

   b. Clarify the reactor types, break size ranges, and break locations for which the parallel channel effect is expected to have a significant impact on statistical predictions of PCT.

RAI-5 Response

It is important to clarify that the sensitivity to [[

]]

The discussion in LTR Section 6.4 describes [[

]] In light of the preceding discussion, the points from the RAI are addressed as follows:

a. To realistically account for [[
]] The detailed core model is described and employed in the responses to RAI-6 and RAI-9. The detailed core model will be used in all plant LOCA calculations.

b. [[
]]

LTR Impact

No changes to the LTR are proposed as the result of this RAI response.

RAI-6

6) Please illustrate the impact of phenomenological uncertainties on the PCT range predicted by the TRACG evaluation model with the parallel channel effect isolated. Please provide a summary of descriptive statistics similar to Figure 6.4-2 for the same case (i.e., BWR/4 limiting break) but with the variability due to the parallel channel effect suppressed and the random variables for PIRT multipliers chosen according to baseline uncertainty distributions. Please further explain the technique used to bias toward prediction of hot channel plugging.

RAI-6 Response

This RAI response is related to the responses for RAI-7 and RAI-9.

During the investigation of this and other related responses, an error was discovered in the analyses presented in Section 6.4. The error was a result of the decay heat range in the [[

]] The conclusions with respect to the [[
]] drawn from the Section 6.4 study, however, remain unchanged. The correction is implemented in the calculations presented in this response.

The original calculations were repeated to establish the correct basis for comparison. Both the [[

]] Figures R6-1 through R6-4 summarize the corrected results.

To illustrate the impact of phenomenological uncertainties on the PCT range predicted by the TRACG evaluation model with the parallel channel effect isolated, two additional sets of analyses were performed. One set of calculations [[

]] These methods are presented here to demonstrate that the large PCT variations shown in Figures R6-1 through R6-4 can be considerably reduced.

In Figures R6-5 through R6-8, the results from the cases with [[ ]] are presented. These figures illustrate the phenomenological uncertainty [[

]] for BWR/4 model is shown in Table R6-1, which can be compared to the LTR channel modeling as shown in LTR Table 8.1-1. As shown in Table R6-1, the changes are [[

]] These results are shown in Figures R6-9 through R6-12. In future applications, GEH plans to utilize the detailed core modeling [[

]] for TRACG LOCA applications.

Table R6-1 TRACG Channel Grouping for Detailed BWR/4 Model

[[					
					]]

[[

]]

Figure R6-1 PCT Range for BWR/4 0.67 ft^2 Break [[ ]]

[[

]]

Figure R6-2 PCT Distribution for BWR/4 0.67 ft^2 Break [[ ]]

[[

]]

Figure R6-3 PCT Range for BWR/4 0.67 ft^2 Break [[ ]]

[[

]]

Figure R6-4 PCT Distribution for BWR/4 0.67 ft^2 Break [[ ]]

[[

]]

Figure R6-5 PCT Ranges for BWR/4 with SEO [[ ]]

[[

]]

Figure R6-6 PCT Distribution with SEO [[ ]]

[[

]]

Figure R6-7 PCT Range with SEO [[ ]]

[[

]]

Figure R6-8 PCT Distribution with SEO [[ ]]

[[

]]

Figure R6-9 PCT Ranges for BWR/4 0.67 ft^2 Break with [[ ]]

[[

]]

Figure R6-10 PCT Distribution for BWR/4 0.67 ft^2 Break with [[ ]]

[[

]]

Figure R6-11 PCT Range for BWR/4 0.67 ft^2 Break with [[ ]]

[[

]]

Figure R6-12 PCT Distribution for BWR/4 0.67 ft^2 Break with [[ ]]

LTR Impact

The following in LTR Section 6.4 (last two paragraphs) will be modified in response to this RAI.

Original

[[

]]

In conclusion, there are inherent uncertainties associated with the modeling. The uncertainty caused by [[ ]] appears to be a dominant contributor to the overall PCT uncertainty. This uncertainty, together with the other computational contributors, can be quantified by [[ ]]
For example, it is known that [[
]] As shown by this example, the standard deviation of the PCT distribution from a statistical analysis [[ ]]
is used to define and calculate the PCT analysis resolution.

Revised

[[

]] Figure 6.4-9 shows the range of PCT and Figure 6.4-10 shows the PCT distribution for different set of cases where the uncertainty parameters are sampled using [[
]] as shown in Figures 6.4-3, 6.4-4, 6.4-7 and 6.4-8 is [[ ]]

In conclusion, there are inherent uncertainties associated with the modeling. The uncertainty caused by [[ ]] appears to be a dominant contributor to the overall PCT uncertainty, which is minimized by using detailed core modeling. This uncertainty, together with the other computational contributors, can be quantified by [[
]] As shown by this example in this section and in the RAI-9 response , the standard deviation of the PCT distribution from a statistical analysis [[ ]] is used to define and calculate the PCT analysis resolution.

[[

]]

Figure 6.4-9 PCT Range for BWR/4 0.67 ft^2 Break with [[ ]]

[[

]]

Figure 6.4-10 PCT Distribution for BWR/4 0.67 ft^2 Break with [[ ]]

RAI-7

7) Please address the following issues associated with the concept of analysis resolution that is outlined in section 6.4 of the TR:

   a. The concept of analysis resolution is meaningful when used in the sense of practical limitations in the capability of an evaluation model to simulate known physical processes in a reactor to an arbitrary degree of precision. However, the linkage in section 6.4 between the analysis resolution and the parallel channel effect does not fully conform to this definition because the probability of bundles containing hot rods in the reactor being plugged with liquid appears to be a significant uncertainty that is fundamentally associated with a limitation in physical knowledge rather than the practical capability of an evaluation model. Therefore, please either redefine the analysis resolution in light of the discussion above, or provide adequate justification for the current approach.

   b. The general method for determining the analysis resolution elaborated in section 6.4 of the TR appears to be predicated on the presumption that, for all potentially limiting LOCA scenarios for operating BWRs, variation in the figures of merit due to [[ ]] that presumably influence the analysis resolution (e.g., nodalization error, time step error, model simplification error). If, however, the limiting LOCA scenario for a given BWR is not [[ ]] Please either generalize the proposed method for determining the analysis resolution, or provide adequate justification for the general applicability of the current approach to all potentially limiting LOCA scenarios for operating BWR designs.

   c. The NRC staff requests additional technical basis to justify the adequacy of a [[ ]] Please use an alternate [[ ]]

   d. Once an appropriate analysis resolution is defined that ensures external factors are bounded, please clarify whether it would be justified to accept a lesser total uncertainty for determining upper tolerance limits (e.g., the standard deviation associated with calculation results). For example, [[ ]]

RAI-7 Response

This RAI response is related to the responses to RAI-6 and RAI-9.

a. GEH agrees with this assessment and has significantly reduced this 'unwanted' uncertainty. The responses to RAI-6 and RAI-9 document that excess non-phenomenological uncertainty can be effectively minimized without artificially biasing the PCT results. In the light of this discussion, the analysis resolution definition is unchanged but now has a much lower value that is easier for the methodology to address.

b. Section 6.4 of the LTR was intended to accomplish two things: (1) introduce the concept that the methodology should address how it treats some level of "noise" that cannot be resolved; (2) identify [[ ]] as an example of "noise" that needed to be addressed by the methodology. As explained in part (a) of this response, the amount of noise has been greatly reduced. As a result, it is now possible to determine contributions to the PCT sensitivity that previously were covered by [[ ]] was being applied. LTR Figures 6.4-7 and 6.4-8 illustrate this point even for [[ ]] Additional discussion of the [[ ]] is provided in part (c) below.

c. The process for determining the analysis resolution has been revised. The [[ ]] Figure R6-11 in the response to RAI-6 and Figure R9-3 in the response to RAI-9 demonstrate the effective convergence of all the PCT traces to the reduced noise level [[ ]]

d. GEH agrees with the implication in part (d) of the request that accepting a total uncertainty for the tolerance limit that is less than the analysis resolution cannot be justified. As explained in the RAI-6 response, an error in the input uncertainty distribution caused a full range sampling of the decay heat in the [[ ]] As shown in RAI-6 and RAI-9 responses, the PCT analysis resolution is now significantly reduced and is now much less than the total uncertainty used in determining the upper tolerance limits.

LTR Impact

No changes to the LTR are proposed as the result of this RAI response. See RAI 6 for the LTR impact of the change in [[ ]].

RAI-8

8) Please provide clarification regarding the process discussed in section 9.2 for determining whether it is necessary to perform a revised statistical analysis in response to a change or error in the evaluation model. The TR states that a [[

]] Please clarify the following points:

a. What is the [[

]]

b. The TR appears to be inconsistent with 10 CFR 50.46, which mandates use of a fixed difference in PCT (50°F) as the criterion for determining whether a cumulation of changes and errors is significant. Given that the 95/95 upper tolerance limit is the regulatory figure of merit, please clarify how the proposed approach complies with 10 CFR 50.46, or revise the approach to ensure compliance.

RAI-8 Response

It is important to understand that 10 CFR 50.46 does not mandate a reanalysis when a change or error in the evaluation methodology is discovered. Instead, an estimate is provided. In most of the cases, the nature of the change would not cause any significant difference in the underlying assumptions and the biases and the uncertainties associated with the methodology. Therefore, the impact can be estimated by various means. Among them, estimation from first principles or known sensitivities, as well as engineering judgment or actual calculations are all valid and allowable methods.

When the impact is estimated using a code calculation, it is also important to recognize that any result within the PCT analysis resolution has equal validity. By comparing the mean values from two sets of PCT resolution analysis [[ ]], the nominal effect of the change or the error can be quantified. If this ΔPCT is within the original PCT analysis resolution (i.e., ≤ the standard deviation of PCT from [[ ]]) computed for the given plant/scenario, then the effect of the change/error would be concluded to be small and not to have significant impact on the validity of the plant calculations done as part of the original analysis. In that case, the ΔPCT would be the quantity used as the estimate reported per 10 CFR 50.46. If the ΔPCT exceeds the analysis resolution, then it would be prudent to evaluate the effect on the upper tolerance PCT. This evaluation would be performed on the limiting break by exercising the full range sampling of the uncertainty contributors to obtain a new upper tolerance PCT. The difference between the newly calculated upper tolerance PCT having the change or correction and the original PCT would be the ΔPCT reported as the estimate of the effect per 10 CFR 50.46. For more significant effects, the latter provides the means of fulfilling the reporting requirements.

This threshold of repeating the full range statistical evaluation is different than the 50°F threshold stipulated in 10 CFR 50.46 for significance. Regardless of the magnitude of the analysis uncertainty, ΔPCT impact arising from a change or an error would be reported according to 10 CFR 50.46 rules, as also indicated in Figure 9.2-1 of the LTR. The concept explained in Section 9.2 of the LTR clarifies how this ΔPCT would be obtained.

In this context,

a. The "statistical analysis" (used in 3rd paragraph of Section 9.2) refers to the PCT resolution analysis [[ ]].
The "full statistical analysis" (used in 4th paragraph of Section 9.2) refers to the case where all the uncertainty parameters are sampled from the full range of their associated distributions. This clarification is added to Revision 1 of the LTR to avoid future confusions.

b. LTR is not inconsistent with the regulation on this aspect of 10 CFR 50.46, since it explains the ways of obtaining the estimate. In the regulation, the fixed 50°F threshold for significance is for 30-day reporting. This threshold is set for either a single change/error effect or the sum of absolute values of the PCT estimates from multiple changes (and/or errors). The regulation requires the licensee to submit the plan for reanalysis in that 30-day reporting. The LTR does not introduce any different notion that is in conflict with these aspects of the regulation. Instead, Section 9.4 provides clarification on how the reportable ΔPCT can be obtained if computer code calculations are used for estimating the impact. This method provides a logical and robust way of determining the effect of a change or an error when there is an inherent computational uncertainty in the calculations, assuring the validity of existing analysis.

LTR Impact

Section 9.2 will be edited as noted in the response above.

RAI-9

9) Please illustrate whether [[

]] the BWR/4 demonstration case. Although general discussion of the topic is provided in section 8.3.2.1 of the TR, based on the information provided in this discussion, the NRC staff could not discern [[

]]

RAI-9 Response

This RAI response is related to the responses for RAI-6 and RAI-7.

The BWR/2 results presented in the LTR are [[

]] Figures R9-1 and R9-2 show the results from such a study.

As indicated in LTR Section 6.4, [[

]] In the actual applications of the methodology, GEH plans to use this improved modeling [[

]]

To demonstrate this point, the BWR/2 core was modeled with additional details. The detailed channel grouping for the BWR/2 model is shown in Table R9-1, which is compared to the LTR channel modeling as shown in LTR Table 8.3-1. As shown in Table R9-1, [[

]] The results are presented in Figures R9-3 and R9-4.

The improved model was also exercised for the full-range uncertainty analysis. These results are summarized in Figures R9-5 and R9-6.

In summary, the BWR/2 results shown in the LTR [[

]]

LTR Impact

No changes to the LTR are proposed as the result of this RAI response.

Table R9-1 TRACG Channel Grouping for Detailed BWR/2 Core Model

[[					
					]]

[[

]]

Figure R9-1 PCT Range for BWR/2 Discharge DBA [[ ]]

[[

]]

Figure R9-2 PCT Distribution for BWR/2 Discharge DBA [[ ]]

[[

]]

Figure R9-3 PCT Distribution for BWR/2 Discharge DBA [[
]]

[[

]]

Figure R9-4 [[
]]

[[

]]

Figure R9-5 [[

]]

[[

]]

Figure R9-6 [[

]]

RAI-10

10) Please provide information similar to that provided in Figure 6.9-5 of NEDE-32177P, Revision 3, for the BWR/4 intermediate and small break time step sensitivity cases presented in Table 5.2-1 of the TR (NEDE-33005P). Please also provide similar information for the BWR/2 discharge Design Basis Accident discussed in section 8.3.2.1 of the TR.

RAI-10 Response

Figure R10-1 shows the time step sensitivity results for the DBA suction break for a BWR/4 with the updated basedeck and latest TRACG code version. This provides a re-baselining as it is a reproduction of the same case shown in Figure 6.9-5 of NEDE-32177P, Rev. 3.

As with the original figure the plot shows [[

]]

[[

]]

Figure R10-1 Time Step Sensitivity for BWR/4 Suction DBA

Figure R10-2 shows the time step sensitivity study performed for an intermediate size suction break (0.67 ft^2). This is the limiting break for the BWR/4 model presented in the LTR. In this break [[

]]

[[

]]

Figure R10-2 Time Step Sensitivity for BWR/4 Intermediate Break

The time step sensitivity results for a representative small break are presented in Figure R10-3. The small break is similar to the intermediate break [[

]] calculated for the intermediate and DBA break sizes.

[[

]]

Figure R10-3 Time Step Sensitivity for BWR/4 Small Break

Figures R10-4 through R10-6 show the timestep sensitivity for the same three break sizes using the detailed average core model (see the description of the BWR/4 detailed core modeling in the response to RAI-6). The time step sensitivity results show no meaningful differences between the detailed and original core model.

[[

]]

Figure R10-4 Time Step Sensitivity for BWR/4 Suction DBA (Detailed Core)

[[

]]

Figure R10-5 Time Step Sensitivity for BWR/4 Intermediate Break (Detailed Core)

[[

]]

Figure R10-6 Time Step Sensitivity for BWR/4 Small Break (Detailed Core)

Similar time step sensitivities were carried out for the BWR/2. Figure R10-7 shows the individual hot channel PCTs in a BWR/2 for the limiting DBA discharge recirculation line break. In the BWR/2 DBA break case the [[

]]

Figure R10-7 also shows that [[

]]

[[

]]

Figure R10-7 Time Step Sensitivity for BWR/2 Discharge DBA

[[

]]

Figure R10-8 Core PCT for BWR/2 Discharge DBA

Reduced sensitivity to changing the maximum time step size is observed [[
]] (See the description of the BWR/2 detailed core modeling in the response to RAI-9.) Figure R10-9 shows the hot channel PCTs as a function of the maximum timestep [[
]] for the BWR/2.

The timestep sensitivity performed using [[

]]

[[

]]

Figure R10-9 Timestep Sensitivity for BWR/2 Detailed Core Model

[[

]]

Figure R10-10 Core PCT for BWR/2 Detailed Core Model

LTR Impact

No changes to the LTR are proposed as the result of this RAI response.

RAI-11

11) Please provide an overview of typical results for the calculated PCT and cladding oxidation from the proposed TRACG evaluation model demonstration analysis as compared to those using the current SAFER evaluation model best-estimate and licensing results for analogous initial conditions.

RAI-11 Response

In this response, the results from SAFER and SAFER/CORCL analyses of similar plants with total core thermal power and ECCS capacities that match the ones used in the LTR demonstration calculations are chosen. Note that the TRACG results show the larger uncertainty band associated with the calculations originally presented in the LTR rather than those calculated later using the more detailed core model as described in the responses to RAI-6 and RAI-9.

It is important to note that the SAFER methodology is not part of the LTR scope and the review and approval of the current LTR is not based on SAFER. Because of these points, no attempt is made to render the analyses more comparable by precisely matching the initial and boundary conditions to the ones used in TRACG calculations. Some noteworthy differences that were not resolved are: (1) different peak linear heat generation rates (PLHGR) used for the TRACG calculations compared to SAFER; (2) GE14 fuel for the TRACG calculations compared to GNF2 for the SAFER calculations for BWR/2 plant type; (3) different small break areas. Because of these differences, the comparisons presented here cannot completely isolate methodology differences. These comparisons are presented for information only and cannot be the basis for determining a degree of conservatism in either method.

Figure R11-1 through R11-4 show the comparisons of PCTs predicted using the SAFER and the TRACG methodologies for similar BWR/4 plant types. Tables R11-1 and R11-2 show the comparisons of the PLHGRs, PCTs and oxidations from these two methods.

The comparisons between SAFER/CORCL and TRACG results for a BWR/2 type plant are also provided. The results are shown in Figure R11-5 and 11-6 and in Table R11-3. Note that the TRACG calculations used a higher PLHGR than the SAFER/CORCL calculation yet the PCT predicted by TRACG was lower than SAFER/CORCL.

LTR Impact

No changes to the LTR are proposed as the result of this RAI response.

Table R11-1 PCT and Oxidation Results Comparison

BWR/4 Large-Break	SAFER	TRACG
Fuel Type	GE14	GE14
PLHGR (1)	[[	
PCT		
ECR		
Break		]]

Note: (1) For SAFER, this value is for Appendix K assumption; for TRACG the nominal value is listed. Those two values do not contain the adders used in the analyses.

Table R11-2 PCT and Oxidation Results Comparison

BWR/4 Small-Break	SAFER	TRACG
Fuel Type	GE14	GE14
PLHGR (1)	[[	
PCT		
ECR		
Break Area (ft^2) (2)		]]

Note: (1) For SAFER, this value is for Appendix K assumption; for TRACG the nominal value is listed. Those two values do not contain the adders used in the analyses.

(2) Small break is for break area ≤ 0.1 ft^2. Reported value is small break area with the highest PCT.

Table R11-3 PCT and Oxidation Results Comparison

BWR/2 Large-Break	SAFER-CORCL	TRACG
Fuel Type	GNF2	GE14
PLHGR	[[	
MAPLHGR		
PCT		
ECR		
Break		]]

[[

]]

Figure R11-1 PCT Results for BWR/4 Large-Break LOCA Using SAFER with App. K Assumptions

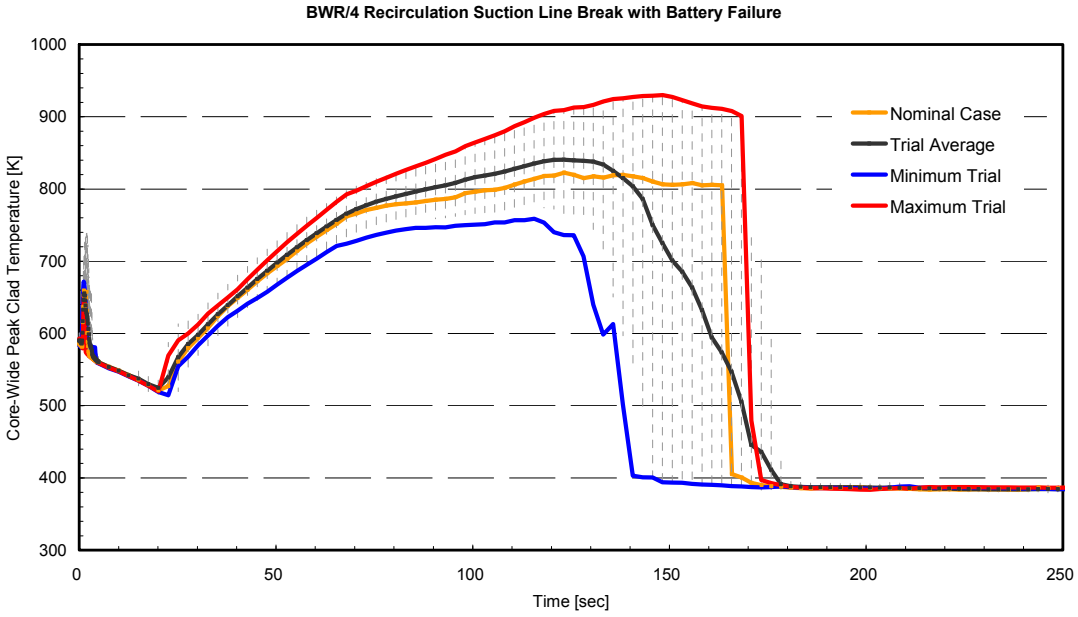

Figure R11-2 PCT Results for BWR/4 Large-Break LOCA Using TRACG

[[

]]

Figure R11-3 PCT Results for BWR/4 Small-Break LOCA Using SAFER with App. K Assumptions.

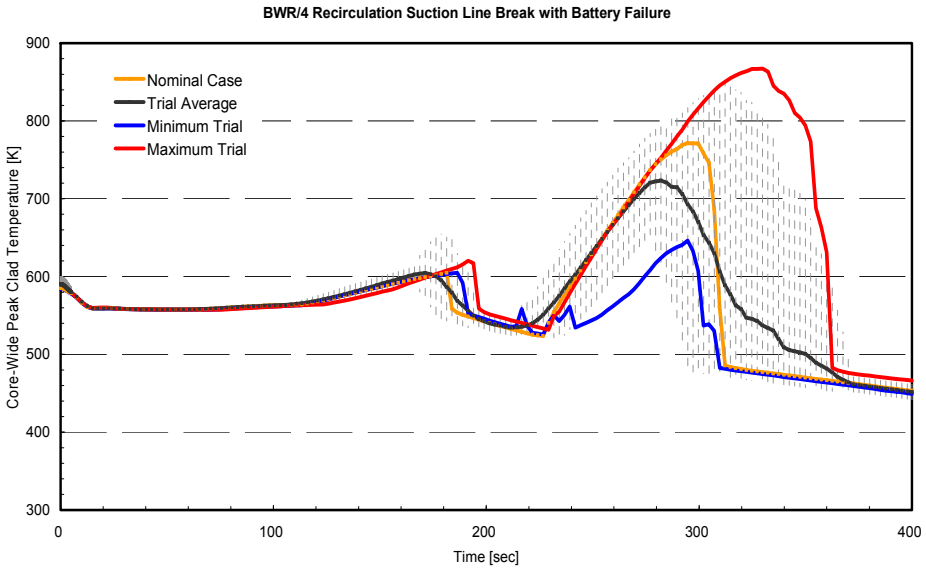

Figure R11-4 PCT Results for BWR/4 Small-Break LOCA Using TRACG.

[[

]]

Figure R11-5 PCT Results for BWR/2 Large-Break LOCA Using SAFER with App. K Assumptions.

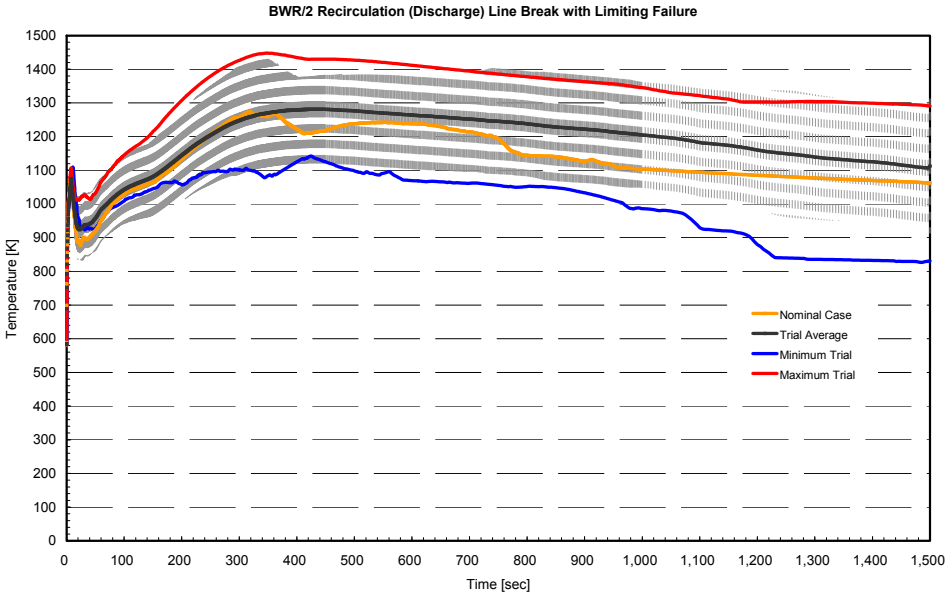

Figure R11-6 PCT Results for BWR/2 Large-Break LOCA Using TRACG

RAI-12

12) Please clarify what assumptions are made concerning offsite power and the availability of nonsafety systems in the demonstration cases and, likewise, how nonsafety systems would be treated for future plant-specific analysis. For example, the small liquid break scenario in Figure 3.2-1 of the TR suggests that reactor pressure is maintained at a control setpoint prior to main steam isolation valve closure, rather than being controlled through the cycling of safety relief valves (SRVs), as indicated in the text of section 3.2.3. An analogous observation is made regarding Figure 8.1-6 and section 8.1.2.2, both of which cases are contrasted with Figure 8.3-17, where SRVs appear to cycle. Please discuss how the availability of offsite power affects the figures of merit for compliance with 10 CFR 50.46 and justify that the assumptions made with respect to offsite power and nonsafety systems are consistent with analyzing the most limiting conditions. Please clarify whether these limiting conditions change as a function of break size.

RAI-12 Response

In the TRACG LOCA application methodology, there is no consideration of any credit gained from non-safety grade systems. This process is unchanged from the current approved LOCA methodology.

[[

]]

In the demonstration cases presented in the LTR, there are some deliberately conservative assumptions regarding Loss of Offsite Power (LOOP) or Offsite Power Available (OPA) conditions. Irrespective of offsite power availability, the SRV operation would have sufficient battery power for the solenoid and/or accumulator gas for the pilot valve to actuate during a small-break LOCA scenario. In safety mode, valve opening and closure does not rely on a power source, unlike in the relief mode.

[[

]]

For small to intermediate break sizes, a LOOP assumption consistent with the plant configuration would provide scram, feedwater trip, and MSIV closure signals concurrently at the beginning of the event. Similarly, OPA assumption consistent with plant configuration would not trip the reactor, feedwater, and MSIVs. The reactor scram would then take place on earlier of L3 or high drywell pressure signals. MSIVs will be signaled to close on L1 or low main steam line (MSL) pressure. When power is available, the feedwater (FW) pumps continue to operate. In this case, the level is maintained for an extended period of time, providing sufficient cooling mitigating any adverse effect of LOCA and practically rendering the small-break event insignificant. The signals for OPA and LOOP assumptions are summarized in Table R12.1. The table also contrasts the assumptions used in the calculations shown in Section 8.

Table R12-1 Assumptions for OPA and LOOP

	OPA Assumption	**LOOP Assumption**	**Demo Calculations**
Scram	L3 or High DW Press.	with LOOP (0 sec)	[[
FW trip	No FW trip	with LOOP (0 sec)	
MSIV trip	L1 or MSL Pressure	with LOOP (~5 sec stroke time to close)	
Recirculation pump trip	L2	with LOOP (conservative time constant for coastdown)	
ADS timer initiation	L1	L1	]]

[[

]]

Table R12-2 Summaries of PCT's for BWR/4 LOCA Runs with current LTR assumptions and with LOOP assumptions

Break Sizes	PCT (K) (From LTR)	PCT (K) From the LTR cases re-run with the Detailed Core Model	PCT (K) From the cases with LOOP run with the Detailed Core Model
[[			
			]]

Figure R12-1 shows one example of the reactor pressure vessel (RPV) pressure responses between the LTR case and the LOOP case (both using detailed core model), which is for the $0.1ft^2$ small liquid line break. [[

]]

[[

]]

Figure R12-1 RPV responses for LTR Figure 8.1-6 case (Current) and the case with LOOP (LOOP), both with Detailed Core Model.

LTR Impact

No changes to the LTR are proposed as the result of this RAI response.

RAI-13

13) [[

]] addressing the following points:

a. [[

]]

RAI-13 Response

The difference in BWR/2 discharge break PCT's between the double-ended guillotine break (DEGB) and the same area split break as shown in Figure 8.3-14 of TRACG LOCA licensing topical report (LTR) is attributed to [[

]]

The PCT time histories for those two cases (called DEGB and Split hereafter) are shown in Figure R13-1. It is observed that the PCT's for both breaks
[[

]]

In summary, the PCT differences for DEGB and the same area split break as shown in LTR Figure 8.3-14 for BWR/2 discharge break

[[

]]

[[

]]

Figure R13-1 PCTs for BWR/2 Discharge Split break and DE GB

[[

]]

Figure R13-2 Air Pressure in the RPV Upper Plenum for BWR/2 Split break and DE-GB

[[

]]

Figure R13-3 PCT for BWR/2 discharge original DE GB and Split break with vent at 160 seconds.

a. Like BWR/2 discharge break, the difference in BWR/2 suction break PCT's
[[

]]

The PCT time histories for those two suction break cases (also called DEGB and Split) are shown in Figure R13-4. It is observed that
[[

]]

[[

]]

Figure R13-4 Core PCTs for BWR/2 Suction DE GB and the same break area Split break

[[

]]

Figure R13-5 Total Air mass inside the RPV for BWR/2 DE GB and the same area split break

[[

]]

Figure R13-6 RPV downcomer water levels (Above Vessel Zero) for BWR/2 Suction DE Gb and the same area split break

[[

]]

Figure R13-7 PCTs for BWR/2 suction original DE GB and Split break with vent at 125 seconds.

b. For the BWR/2 discharge break, the limiting break is the DEGB, with a core PCT [[

]]

These results together with the sensitivity studies described in part (a) of the response show that [[

]]

c. As discussed in the response to this RAI, [[

]]

The responses above were discussed in a meeting on July 1, 2013. The additional information provided below is in response to questions asked by the NRC staff at the July 1, 2013 meeting.

Regarding BWR/2 Break Locations

[[

]]

Regarding the BWR/2 Detailed Core Modeling (discussed in RAI-9)

The TRACG runs performed above for this RAI response are based on the same TRACG model as presented in the LTR. [[

]]

Regarding Intermediate Break

[[

]]

LTR Impact

No changes to the LTR are proposed as the result of this RAI response.

RAI-14

14) The TR indicates in section 3.4 that medium-ranked parameters have a small effect on primary safety parameters and may be excluded in the overall uncertainty evaluation. This definition and treatment is not consistent with the typical characterization of medium-ranked parameters as those having a moderate effect on figures of merit (i.e., neither dominant nor negligible). The NRC staff further noted that the demonstration analyses presented in section 8.1.3 appear to include several medium-ranked parameters among the most influential for determining PCT.

a. Please confirm whether medium ranked parameters will be included in statistical analysis and revise the TR (e.g., section 3.4) as necessary to be consistent with the positions taken in this RAI response.

b. Please confirm whether future plant-specific analyses will be based on the use of the highest overall rank for a given PIRT phenomenon versus design-specific / scenario-specific PIRT rankings. This distinction is important because, while the NRC staff agrees that the design- and scenario-specific PIRT rankings in the TR are largely representative of typical BWRs of a given product line, it is not clear that they fully capture design variations among individual plants (e.g., certain BWR/3s and /4s with elevated PCTs).

RAI-14 Response

There are no medium-ranked phenomena that were excluded in the overall uncertainty evaluation. All high and medium ranked parameters are included consistent with all previously approved TRACG application methodologies.

a. This response to the RAI formally confirms that the medium-ranked parameters are and will be included in statistical analysis along with the highly ranked parameters. In Revision 1 of NEDE-33005P, Section 3.4 is revised accordingly.

b. This response to the RAI also confirms that plant-specific analyses will be based on the use of the highest overall rank for a given PIRT phenomenon versus design-specific (i.e., BWR/2, BWR/3-4, or BWR/5-6) and scenario-specific (small- or large-break LOCA) PIRT rankings. However, this confirmation does not constitute a new commitment to performing a PIRT evaluation in future applications. The Phenomena Identification and Ranking Table (PIRT) presented in Section 3 extensively covers all design- and scenario-specific rankings for all BWR types having either external recirculation pumps or jet pumps. The design variations among individual plants do not surmount to differences that depart from one particular product line, and hence, do not necessitate generation of plant-specific PIRT. The PIRT process is presented generically as part of the methodology review.

LTR Impact

LTR Section 3.4 will be revised to state that all high and medium ranked parameters are included.

RAI-15

15) The technical basis for the uncertainty distribution and justification GEH proposed for PIRT item M9 (LPCI/Break Flow Interaction) was not apparent to the NRC staff. In particular, the discussion in section 5.1.12.5 proposes that [[

]] However, other factors would apparently influence this phenomenon, such as local flow conditions, the assumed break orientation and geometry, and nodalization. Therefore, please provide adequate justification to support credit taken for LPCI flow from the broken loop to the core across the spectrum of breaks for which this flow would be split between the break and the vessel. To the extent possible, please include reference to experimental data that can be used to validate the flow splits predicted by the TRACG evaluation model.

RAI-15 Response

The sentence in Section 5.1.12.5 stating "The interaction between LPCI and break flow is controlled by the liquid-side interfacial heat transfer." will be replaced with the sentence "Interfacial heat transfer of cooler LPCI water injected into the recirculation line with steam in the line influences the calculated pressure gradient in the line which in turn influences the break flow." With respect to what fraction of the LPCI flow gets into the vessel versus flowing out the break, there are several other more important considerations that are discussed in this response. First an explanation is provided for how LPCI interaction with the break location is modeled so that LPCI fluid into the vessel from the broken loop will not be overestimated. Then, the role played by interfacial heat transfer is described in its proper context.

The concern in the RAI is limited to BWR/3s and some BWR/4s where LPCI is injecting into the recirculation loop. External pump plants (BWR/2s) do not employ LPCI. For the newer BWR/4s and all BWR/5s and BWR/6s, LPCI is directly injecting to the core bypass region inside the core shroud. For larger breaks in those plants that could be affected, all LPCI sweeps out from the break and is discharged out of the system before reaching the vessel. Therefore, the issue as described is only of concern for small break scenarios in some of the plants.

No undue credit is gained from the LPCI for the affected plants. The pump discharge break location for plant designs with LPCI injection into the recirculation line is modeled between the LPCI connection point and the reactor vessel so that the flow of LPCI water out the break is favored. In the case of pump suction break, LPCI flow toward the vessel is retarded because the pressure gradient is directed away from the vessel back toward the break. How much LPCI water makes it into the reactor vessel is determined by this pressure gradient which depends on the assumed size of the break.

There is no stratification in the recirculation line because the model for the line is one-dimensional; break orientation, shape and geometry of the break have no meaning in such a model. Sampling of the break flow uncertainty addresses any relatively small effects of shape and orientation over the break geometry. Any larger effects are covered by analysis of different break sizes.

The only potential interaction in the modeling is related to the mixing of the two flows: break flow from the vessel side and the colder coolant from the injection. [[

]] This is also demonstrated in the response to RAI-34. The sensitivity runs performed as part of RAI-34 response indicate that LPCI mixing impact is not significant in LOCA analysis.

LTR Impact

LTR Section 5.1.12.5 will be revised as indicated above.

RAI-16

16) Please clarify whether TR reference [46] is consistent with the assertions in section 5.1.2.4 that [[

]]. Because of the significant difference in [[

]] is unclear.

RAI-16 Response

[[

]]

The sample calculations are performed for a BWR/4 intermediate break ($0.67ft^2$). [[

]] These comparisons show that the choice of guide tube-bypass CCFL inputs given in the LTR for TRACG LOCA application is reasonable.

LTR Impact

No changes to the LTR are made as the result of this RAI response.

Table R16-1 Statistical Core PCT Summary

[[				
				]]

[[

]]

Figure R16-1 Comparison of Guide-bypass CCFL Ranges

Note for Figure R16-1:

[[

]]

[[

]]

Figure R16-2 Core PCTs for ORIGINAL Runs [[ ]]

[[

]]

Figure R16-3 Core PCTs for PIRT Runs (NEDE-30996P[[ ]]

RAI-17

17) Please clarify the nomenclature regarding lognormal distributions that is used throughout the TR.

a. Please confirm what is meant by mode and gain when referring to the lognormal distribution. For example, see Figure 5.1-10, where the reported mode does not appear to correspond to the peak of the probability distribution function.

b. Please confirm whether, in the discussion of PIRT item A1, it is correct that the quoted standard deviation of [[ ]] belongs to the associated normal distribution, rather than the lognormal distribution being discussed.

RAI-17 Response

The definitions of **gain** and **mode** for log-normal distributions are given below. The NRC expectation is that **mode** should correspond to the peak of the probability distribution is correct. Figure 5.1-10 in the LTR is incorrect and will be replaced as indicated in the response to RAI-40. The discussion of a standard deviation for PIRT item A1 in the LTR will be removed since it is extraneous. As shown below, the mode and gain fully specify the log-normal distribution and from this specification other statistics of the random variable X can be calculated.

A log-normal probability density function (PDF) is defined by

$$f(x) = \frac{1}{\sqrt{2\pi}x\sigma_{\ln x}} \exp\left[-\frac{1}{2\sigma_{\ln x}^2}[\ln(x) - \mu_{\ln x}]^2\right], \text{ for } \{x,\ \sigma_{\ln x}\} \quad \text{(R17-1)}$$

where

x is the value of a positive random variable X with a log-normal distribution,

$\mu_{\ln x}$ is the mean of the of the random variable X,

$\sigma_{\ln x}$ is the standard deviation of the $\log_e$ of the random variable X.

In the TRACG LOCA application, the working range for the PDF is selected to be a 3σ on either side of the x_m, which is the value of x where the frequency $f(x)$ is the maximum. The value for the mode x_m can be found by differentiating Eq. R17-1 and solving such that

$$f'(x_m) = 0 \quad \text{(R17-2)}$$

It follows x_m, $\sigma_{\ln x}$ and $\mu_{\ln x}$ are related to each other by

$$\mu_{\ln x} = \sigma_{\ln x}^2 + \ln(x_m) \quad \text{(R17-3)}$$

$$x_m = \exp(\mu_{\ln x} - \sigma_{\ln x}^2) \quad \text{(R17-4)}$$

The mode x_m of the log-normal PDF is of interest because **the intended application is to simulate a log-normal PDF where the mode x_m is given. What is needed is a way to define either $\sigma_{\ln x}$ or $\mu_{\ln x}$ such that the specified value of x_m will be realized.** One way of doing this is to relate $\sigma_{\ln x}$ to the expected working range for the PDF. For 95% probability and 95% confidence in a two-sided normal distribution requires a working range of at least $\pm(1.960*1.217)\sigma$ on either side of the mean for sixty or more samples. In other words for a set of 60 values {y} from a normal distribution, a working range of $[y_1, y_2]$ where

$$y_1 = \mu - 2.38532\sigma \tag{R17-5}$$

$$y_2 = \mu + 2.38532\sigma \tag{R17-6}$$

is sufficient to assure with 95% probability and 95% confidence that any other sample will be inside the range. Choosing a broader (more conservative) $\mathbf{6\sigma}$ span for the working range $\mathbf{[y_1, y_2]}$ leads to

$$y_1 = \mu - 3\sigma \tag{R17-7}$$

$$y_2 = \mu + 3\sigma \tag{R17-8}$$

and

$$\sigma = \frac{1}{6}(y_2 - y_1) \tag{R17-9}$$

This larger range with a $\mathbf{6\sigma}$ span provides approximately 97.5% probability and confidence for a sample size of sixty. To relate this working range $\mathbf{[y_1, y_2]}$ for the normal distribution to the working range $\mathbf{[x_1, x_2]}$ for the log-normal distribution apply the relationship

$$\{y\} = \ln(x) \tag{R17-10}$$

to write

$$\sigma_{\ln x} = \frac{1}{6}(y_2 - y_1) = \frac{1}{6}[\ln(x_2) - \ln(x_1)] = \frac{1}{6}\left[\ln\left(\frac{x_2}{x_1}\right)\right] \tag{R17-11}$$

At this point it is convenient to introduce the concept of a "gain", **g**. For convenience the gain is defined about the mode such that the working range for the underlying normal PDF has minimum and maximum values defined by

$$x_1 = \frac{x_m}{\mathrm{g}} \tag{R17-12}$$

$$x_2 = x_m \mathrm{g} \tag{R17-13}$$

It is obvious that $\mathbf{g} \neq 0$ and to make physical sense it is necessary that $\mathbf{g} \geq \mathbf{1}$. It is also apparent that for $\mathbf{g} = \mathbf{1}$ that $\boldsymbol{x_1} = \boldsymbol{x_m} = \boldsymbol{x_2}$ and that all three values must always be greater than zero. Another useful relationship that follows from Eqs (R17-12) and (R17-13) is

$$\mathbf{g} = \sqrt{\frac{x_2}{x_1}} \tag{R17-14}$$

When the relationship between **g** and $\frac{x_2}{x_1}$ is applied to Eq. (R17-11) one gets

$$\sigma_{\ln x} = \frac{1}{6}\left[\ln\left(\frac{x_2}{x_1}\right)\right] = \frac{1}{6}[\ln(\mathrm{g}^2)] = \frac{1}{3}\ln(\mathrm{g}) \tag{R17-15}$$

LTR Impact

Figure 5.1-10 will be revised.

LTR Section 5.1.1.1 will be revised as follows:

Flashing and the associated redistribution of liquid inventory in the lower plenum of the TRACG model are controlled by liquid-side interfacial heat transfer. The bubbly flow regime is the dominant flow regime for this behavior. TRACG uses the Lee-Ryley correlation in conjunction with a bubble diameter based on a critical Weber number for liquid-side heat transfer in the bubbly flow regime [1]. The Lee-Ryley correlation applies to heat transfer to spherical particles under forced circulation conditions. It predicts the water droplet evaporation data from which it was originally developed with an error less than 10%. Following the procedure previously adopted for the Anticipated Operational Occurrences (AOO) application [3], the uncertainty in the PIRT multiplier on the interfacial heat transfer at the bubble surface is specified as a [[

]]

RAI-18

18) Please address the following issues with the statistical distribution for PIRT item F1 by revising the statistical distribution or providing adequate justification for the current approach:

a. Representation of the void deviation using [[
]]

b. It is unclear that the distribution parameters and imposed cutoff capture data at both the upper and lower extremes of the distribution (Is the minimum of [[ ]] samples reasonably considered the minimum possible value of the distribution?).

c. The selection of a [[
]] inflate the expectation value of the multiplier.

RAI-18 Response

(a) The [[ ]] associated with the void deviations for tests applicable to regions with large hydraulic diameter was only obtained from the Anderson-Darling normality test. Other statistical tests yield a [[ ]] indicating that it would not be unreasonable to assume [[

]] was used for PIRT item F1. The sentences of "[[
]]" in LTR Section 5.1.6.1 are deleted. See the discussion in the response to RAI-19.

(b) The comparisons are directly obtained from TRACG calculations. The deviation of the predicted void fraction from measured data is well represented by the range of the data used in derivation of the uncertainty parameter. As indicated in Section 5.1.6.1 of the LTR, the individual deviations for the TRACG predictions of the data sets used to establish the void fraction uncertainty were in no case greater than [[ ]] and the maximum deviation between all predictions and the void data was [[ ]] indicating that no more extreme points would be anticipated. The current LTR PIRT F1 used [[ ]] data samples. In the response to RAI-19, more data samples have been used for this PIRT item. A refined PIRT F1 uncertainty is presented. The probability density function (PDF) is presented in RAI-19 response to bound all [[ ]]

(c) Application of the [[ ]] amplifies the impact on the expectation value of the multiplier, especially at the extremes. In contrast, [[
]] this possible inflation, making it more in line with physical reality. This is further demonstrated in the response to RAI-19, in which the [[

]](See Response to RAI-17 Equation R17-12).

LTR Impact

The LTR change with this RAI is made in RAI-19.

RAI-19

19) Please explain and justify the criteria used for selecting test data for the uncertainty derivations for PIRT item A5 (lower plenum void distribution) and related PIRT item F1 (upper plenum void distribution). Different selections of data from some of the same test facilities (9 tests for A5 versus 28 tests for F1) were made to derive the respective uncertainty distributions.

RAI-19 Response

The discerning factors for limiting the experimental void fraction data for determining the lower plenum void distribution uncertainty (PIRT A5) only to the five Wilson data points and the four Bartolomei data points are: [[

]] (as seen from NEDE-32177P, R3 Section 3.1.3). The relevant discussion from Section 5.1.1.6 of the LOCA LTR is quoted below:

"[[

]]... "

Note that the label for Figure 5.1-2 is incorrect. The sensitivity study that is pictured was determined from the [[ ]] model and data.

For determining the void distribution and two-phase level uncertainty for the upper plenum (PIRT F1), [[

]]

LTR Impact

Figure 5.1-2 label will be corrected as

Sensitivity of TRACG Prediction of Average Void Fraction in Large Hydraulic Diameter Test Facilities to PIRT Multiplier

LTR Section 5.1.6.1 will be updated as follows.

5.1.6.1 F1 – Void Distribution/Two-Phase Level (H)

[[

]] These data are characterized by their applicability to the prediction of void fraction in regions with relatively large hydraulic diameter. Accordingly, selections from this data set, taking into consideration other aspects of the test conditions, will be used as the basis for defining the [[ ]] A statistical summary of the comparisons of TRACG predictions with measurements from these four data sets, combined as a single set of deviations, is shown in Figure 5.1 20. The absolute mean bias is [[ ]] void and the absolute standard deviation is [[ ]] void.

[[

]] (A comparable evaluation for lower plenum is described under A5 in Section 5.1.1.6 and for the core and bypass is described below under C2AX in Section 5.1.3.3.)

[[

]]

LTR Table 5.1-2 will be updated as follows and Figures 5.1-20 and 5.1.22 will be updated with Figures R19-1 and R19-2.

[[

]]

Figure R19-1 Void Fraction Deviations for Tests Applicable to Regions with Large Hydraulic Diameter

[[

]]

Figure R19-2 Probability Distribution for Multiplier on Interfacial Drag Coefficient

RAI-20

20) In a number of demonstration cases in the TR, the PCT calculated for the limiting bundle [[

]] (e.g., Figures 8.1-5, 8.1-23, 8.1-24, and 8.1-25).

a. [[

]]

b. In cases where the maximum PCT occurs in a Ring 2 bundle, it does not appear to [[ ]] as discussed in section 5.1.6.4, [[ ]] Please provide an alternate justification that the spray flow distribution uncertainty is bounded in this case.

RAI-20 Response

This RAI response is related to the response for RAI-21.

a. During the post-blowdown phase of a large-break LOCA, the liquid that was present in the fuel channel would be almost entirely depleted either by flowing and draining out of the assembly or by flashing. As the rods dry out, the main heat transfer mechanism would be convection and radiation. Convective heat transfer by steam is the dominant cooling mechanism until sufficient amount of coolant penetrates the channel and the cladding surface temperature eventually drops down below the minimum stable film boiling temperature, allowing rewet. During this period, the magnitude of steam cooling is a strong function of the amount of steam available and its velocity. [[

]]

As the coolant forms a pool in the upper plenum, the amount of liquid that drains into the channel is governed by Counter Current Flow Limitation (CCFL) and can be further limited.

b. The uncertainty in the spray distribution, as discussed in Section 5.1.6.4 of the LTR is related to [[

]]

LTR Impact

No changes to the LTR are proposed as the result of this RAI response.

RAI-21

21) PIRT item F4 in section 5.1.6.4 discusses the spray distribution for an uncovered upper plenum.

a. Please clarify whether [[

]]

b. Please clarify GEH's position concerning whether the specific information contained in TR section 5.1.6.4 is applicable only to [[ ]] or all BWR/2s.

c. Please provide TR references [64] and [61].

d. Please clarify whether spray degradation is primarily a function of reactor pressure or the differential pressure between the reactor vessel and wetwell. Please identify the wetwell pressure assumed in the calculation.

RAI-21 Response

This RAI response is related to the response for RAI-20.

a. [[

]]

b. As indicated Section 5.1.6.4, [[

]]

c. The requested references will be delivered to the staff.

d. Spray degradation is primarily a function of the differential pressure between the vessel and the wetwell. However, [[

]]

LTR Impact

No changes to the LTR are proposed as the result of this RAI response.

RAI-22

22) Please provide justification for ranking [[
]] The TR notes that choking may occur at the jet pump for large discharge breaks, and this behavior is exhibited in the demonstration calculations in Chapter 8. The demonstration calculations also indicate that discharge breaks may be limiting for some BWRs.

RAI-22 Response

In the PIRT process, the phenomena are ranked according to their relative influence on the LOCA critical parameters. [[

]] Although a relative ranking given to a particular physical aspect is somehow subjective and open to debate, the outcome does not change. It is also acknowledged that one particular PIRT item, [[ ]], might be more important than [[ ]] However, the coarse assignment of rankings, such as H-M-L, does not permit discerning these differences.

Jet pump flow reversal and two-phase conditions in the jet pumps occur in early blowdown phase of a large-break LOCA. In smaller breaks, a milder initial flow transient would occur. As flow reversal in jet pumps on the broken loop side happens, choking at the jet pump nozzle will happen. These phenomena, including the expected behavior of jet pump flow, are modeled in the LOCA analyses as they are exhibited, and the biases and uncertainties associated with each of these phenomena are included in the calculations.

LTR Impact

No changes to the LTR are proposed as the result of this RAI response.

RAI-23

23) The NRC staff was unable to confirm the statistical distributions proposed for certain parameters from either Table 5.1-2 or the text of Chapter 5 (e.g., PIRT items A2, A3 (wall heat transfer), C20 (minimum stable film boiling temperature), Q5, C22, L3, M8, G3). Please explicitly identify the statistical distributions proposed for any parameters if not previously provided.

RAI-23 Response

The subsections in LTR Section 5.1 provide the uncertainty treatment for each phenomenon that is ranked high or medium. Either the distribution for the parameter that affects the uncertainty is provided or, if another parameter already covers the particular uncertainty or a different treatment is applied to address the uncertainty, an explanation is provided. Section 5.1 of the LTR provides complete accounting of model uncertainties that are considered in the TRACG LOCA methodology. All the uncertainty parameters listed in LTR Table 5.1-2 have normal distribution, unless noted otherwise in the comments column. The log-normal distributions are expressed with defining parameters given in parentheses. The LTR Table 5.1-2 will be updated to denote all normal distributions to eliminate ambiguity. Following items referred in the RAI, are listed with additional clarification:

A2 – heat slab stored energy release is controlled by wall heat transfer. A multiplier is applied to wall heat transfer coefficient. In the statistical analyses, the multiplier is [[

]], as stated in Section 5.1.1.2 and Table 5.1-2 of the LTR.

A3: The two-phase level and SEO uncovery timing are affected by [[

]].

C20: The uncertainty applied to the minimum stable film boiling temperature T_{min} is [[

]] See the response to the RAI-50 for updated discussion on C20.

Q5: The uncertainty of isolation condenser heat removal capacity was originally considered as a multiplier on the secondary side heat transfer with a large range around the nominal value. However, as indicated in Table 5.1-2, a bounding approach is taken in BWR/2 analyses and no IC is modelled. Therefore, there is no applicable uncertainty. As also committed in RAI-62 response, a heat transfer uncertainty model will be considered only if IC is modeled.

C22: Channel to bypass heat transfer uncertainty is treated by multipliers on the heat transfer coefficients of the channel inside and outside surfaces. The multiplier applied to inside channel wall heat transfer model [[

]] (LTR Section 5.1.3.28). The multiplier on the outside is same as A2 and it has an uncertainty [[ ]] (LTR Section 5.1.1.2). These parameters are listed in LTR Table 5.1-2.

L3: Although not a dominant factor in recirculation line breaks, the uncertainty of steam line pressure drop is applied as a multiplier on the local losses that is sampled from [[

]] (LTR Section 5.1.11.3 and Table 5.1-2). This uncertainty is the same value from the approved Anticipated Operational Occurrences (AOO) application (Reference R23-1).

M8: Similar to L3, the pressure drop in recirculation line has [[ ]] that was specified on the basis of comparisons between TRACG predictions and pressure drop data, as indicated in LTR Section 5.1.12.4 and Table 5.1-22.

G3: As explained in LTR Section 5.1.7.2 and given in Table 5.1-2, the reverse flow characteristics of a jet pump can be varied by [[

]]

Reference

R23-1 NEDE–32906P–A, "TRACG Application for Anticipated Operational Occurrences Transient Analyses," Revision 3, September 2006.

LTR Impact

As indicated in the response, the LTR Table 5.1-2 will be updated to denote all normal distributions.

RAI-24

24) Please confirm that the TRACG LOCA evaluation model will require fuel parameter inputs from the PRIME code, and that code options associated with fuel thermal conductivity degradation will be implemented in a manner that addresses NRC staff concerns expressed in its letter dated March 23, 2012 (Agencywide Documents Access and Management System (ADAMS) Accession No. ML120680571). If approval for inputs from legacy fuel codes (e.g., GESTR is referred to in the TR) or legacy TRACG code options is requested, please provide justification.

RAI-24 Response

As noted in the NRC's Safety Evaluation in Reference R24-1, "in accordance with IMLTR Limitation 12 and Supplement 3, GEH intends to use PRIME T-M methods for future applications". GEH is not seeking approval for inputs from legacy fuel codes (e.g., GESTR) or legacy TRACG code options that invoke such models or inputs as part of the TRACG LOCA evaluation model. The TRACG LOCA application methodology uses only the PRIME-based thermal conductivity model together with fuel parameter inputs supplied by the PRIME code to address the NRC staff concerns associated with fuel thermal conductivity degradation.

Reference

R24-1 NEDC-33173P-A, Revision 4, "Applicability of GE Methods to Expanded Operating Domains," November 2012.

LTR Impact

References to the GESTR thermal-mechanical model will be removed from LTR Table 2.5-1 so that PRIME is indicated as the only option.

RAI-25

25) Please clarify the behavior in Figure 8.1-5, wherein [[

]] as stated in section 8.1.2.1. Nor does the difference appear to be primarily associated with the timing of reflood, since the divergence in temperature seems to originate approximately coincidently with the start of low-pressure core spray (LPCS).

RAI-25 Response

The TRACG BWR/4 DBA run used to produce LTR Figure 8.1-5 was reviewed to determine the axial nodes where the channel PCT occurs. [[

]]

This DBA case was re-run with the graphical data saved in a much smaller time interval after the first 5 seconds of the transient (0.2s now versus 2.5s originally). Also, additional graphical information was obtained for the nodes where the channel PCTs were observed. The PCTs for those channels shown in LTR Figure 8.1-5 are presented in Figure R25-1. Note that the average channel results have been dropped from the figures in this RAI response since they are irrelevant. Comparisons between LTR Figure 8.1-5 and Figure R25-1 show that the overall behavior for each channel for the re-run is comparable to the original result.

Figures R25-2 and R25-3 show the void fraction and steam temperature at the PCT nodes for [[

]] as shown in Figure R25-1 and also with more detail in Figure 25-4. This divergence in heat up rates [[

]] as shown in Figures R25-2 and R25-3.

The NRC reviewer has correctly observed that
[[

]] as shown in Figure R25-4. The sentence stating "The CPR-limited bundles, which are outlet peaked, heat up earlier and subject to the highest PCTs" in LTR Section 8.1.2.1 will be replaced with
"[[

]]"

LTR Impact

The sentence stating "The CPR-limited bundles, which are outlet peaked, heat up earlier and subject to the highest PCTs" in LTR Section 8.1.2.1 will be replaced with
"[[

]]"

[[

]]

Figure R25-1 PCT for Various Channels for BWR/4 Suction DBA

[[

]]

Figure R25-2 Void Fraction at PCT Nodes in Various Channels for BWR/4 Suction DBA

[[

]]

Figure R25-3 Vapor and Saturation Temperatures at PCT Nodes in Various Channels for BWR/4 Suction DBA. [[

]]

[[

]]

Figure R25-4 PCT for Various Channels for BWR/4 Suction DBA (Part of Figure R25-1)

RAI-26

26) Comparing Figures 8.1-6 and 8.1-7 (BWR/4 small-break LOCA), cladding temperatures appear to turn around rapidly following initiation of LPCS (even Ring 1 bundles), despite only faint quantities of core spray being injected prior to 300 seconds. Please explain this behavior and contrast it with the scenario analyzed in Figures 8.2-6 and 8.2-7 (BWR/6 small-break LOCA), where larger LPCS flows over approximately 30 seconds are unable to arrest the PCT transient.

RAI-26 Response

The BWR/4 small break (0.1 ft^2) case presented in LTR Figures 8.1-6 and 8.1-7 has been reviewed, and it has been determined that [[

]]

This BWR/4 case from the LTR was re-run to obtain additional graphical results to facility better understanding of the results. Key results similar to those presented in LTR Figures 8.1-6 and 8.1-7 are shown in Figure R26-1.

[[ ]]

Figure R26-2 presents the results from a modified case for this break. All the inputs for this modified case are the same as the original case with only one change,

[[

]]

The comparison of results shown in Figures 26-1 and 26-2 demonstrates that [[

]]

The following wording in the third paragraph of LTR Section 8.1.2.2:

"The heatup is terminated following the refill of the lower plenum and core by the ECC system. The outlet peaked CPR-limited bundles earlier than the LHGR-limited bundles and experiences the highest PCTs."

will be revised to

"The heatup is **usually** terminated following the refill of the lower plenum and core by the ECC system.
[[

]]"

LTR Impact

The third paragraph in LTR Section 8.1.2.2 will be revised as discussed above.

[[

]]

Figure R26-1 PCTs for Various Channels for BWR/4 Small Break and CS, LPCI and Feedwater Flow. This is the re-run of LTR Figures 8.1-6 and 8.1-7 case with no changes.

[[

]]

Figure R26-2 PCTs for Various Channels for BWR/4 Small Break and CS, LPCI and Feedwater Flow. For this case [[
]], compared to the case in Figure R26-1.

[[

]]

Figure R26-3 PCTs for Various Channels for BWR/6 Small Break and CS, LPCI and Feedwater Flow. This is the re-run of LTR Figures 8.2-6 and 8.2-7 case with no changes.

[[

]]

Figure R26-4 PCTs for Various Channels for BWR/4 Small Break and CS, LPCI and Feedwater Flow. For this case [[

]] in Figure R26-1.

RAI-27

27) The demonstration cases in Chapter 8 refer to the MELLLA+ power-flow map to establish limiting conditions for the analysis basis of BWR/4 and BWR/6 reactors. For plants that do not use this map, please clarify how the limiting power and flow conditions will be determined.

RAI-27 Response

The demonstration cases presented in Chapter 8 are for illustrative purposes only. The power-flow map assumed in the demonstration cases is not presented as a generic map to be used to establish the limiting conditions for the analysis basis. Each application will use the plant-specific power-flow map and determine the power-flow condition that leads to the highest PCT.

LTR Impact

No changes to the LTR are proposed as the result of this RAI response.

RAI-28

28) Based on Figure 8.1-10 in the TR, the limiting condition for axial flux peaking appears to depend on fuel-specific factors, such as the extent to which partial-length rods are present. Please clarify whether differences in fuel and/or plant design would be accounted for in the determination of the limiting axial flux profile used for plant-specific LOCA applications, or whether GEH considers node [[ ]] to be generically limiting for axial flux peaking. The NRC staff notes that node [[ ]] was considered to be the limiting axial flux peaking location for all TR demonstration calculations, apparently based on the analysis in section 8.1.4.2.

RAI-28 Response

In the LTR demonstration cases, node [[ ]] is the node with highest LHGR for the top-peaked axial power shape bundles. Depending on the bundle design, the location of the peak yielding the highest PCT can vary. Among the factors affecting the limiting condition are partial rod configuration, enrichment and burnable absorber concentration in each rod, and bundle exposure. For a top peaked power shape, [[

]]

GEH will consider peak locations in the axial power shapes that are sufficiently bounding. The location of the peak used in the future applications will be consistent with the fuel design. For future fuel types, bundle design changes will be evaluated and power shape assumptions for bounding top and bottom peaks will be reevaluated.

LTR Impact

No changes to the LTR are made as the result of this RAI response.

RAI-29

29) Similar to what has been provided for the BWR/4 in Table 8.1-5, please present results for sensitivity studies for BWR/2 axial peaking for the PCT and maximum local oxidation to confirm that the limiting axial flux profile has been identified. For example, it is unclear to the NRC staff that a [[

]]

RAI-29 Response

The sensitivity of the transient behavior of the limiting BWR/2 break to axial power shapes was performed to evaluate the effect on peak cladding temperature (PCT) and equivalent cladding reacted (ECR). Such a sensitivity study follows a two-step process, wherein first the PCT and ECR are evaluated for the different hot channels in the core for the reference case, and second the elevation of the peak node in the limiting hot channel is varied in full-range CSAU analyses to identify the most limiting shape.

Table R29-1 shows the maximum PCT and ECR for the hot channels in the BWR/2 model with detailed average channel grouping (see response to RAI 9) for the limiting break scenario. [[

]]

With the [[ ]] bundle identified as the appropriate limiting channel type, several sensitivities were performed which moved the peak axial power node position. The additional power shapes considered are summarized in Figure R29-1. Each power shape is evaluated [[
]].

The results in Tables R29-2 and R29-3 demonstrate that [[

]]

[[

]]

Table R29-1 BWR/2 DBA Discharge Break Scenario

[[				
				]]

Note [1]: The overall maximum values presented here are larger than all of the average values presented for individual channels. This is expected because the channel that sets the overall maximum can vary on a case-by-case basis.

[[

]]

Figure R29-1 BWR/2 Axial Power Shape Sensitivity

Table R29-2 BWR/2 PCT Sensitivity to Peak Node in [[
]]

[[		
		]]

Table R29-3 BWR/2 ECR Sensitivity to Peak Node in [[
]]

[[		
		]]

LTR IMPACT

No changes to the LTR are proposed as the result of this RAI response.

RAI-30

30) Please explain the [[

]] for the BWR/4 case shown in Table 8.1-12. Further, although the upper bound ECCS coolant temperature considered seems relatively high, based on Figure 8.3-15, it is not clear that exceeding the nominal ECCS coolant temperature would not adversely impact cladding oxidation for a BWR/2. Please further discuss the influence of ECCS coolant temperature on oxidation for the BWR/2 (with emphasis on the limiting scenario) and adequately justify the choice of the limiting condition chosen.

RAI-30 Response

BWR/4

The results presented in Table 8.1-12 of the LTR originated from single-case sensitivity studies. An effect of using single-case studies is that the resulting sensitivity is a function not only of the parameter being varied, but also of the inherent code uncertainty, which can drive the PCT result upward or downward within the analysis resolution of the model. In the case of the LTR ECCS temperature sensitivity, the single-case comparison method [[

]].

This apparent trend is not characteristic of the actual sensitivity of the model. The true sensitivity of the limiting BWR/4 break model with detailed average channel grouping (see response to RAI 6) to bounding ECCS temperatures was assessed using [[

]], such as those presented in the response to RAI 29. Here, the ECCS temperature is set to the bounding high and low values used in the original demonstration presented in Table 8.1-12 of the LTR.

The results of the sensitivity calculation using the low and high pool temperatures are presented in Table R30-1. It is shown from these results that [[

]]. It is therefore concluded that [[ ]] is a defendable input for ECCS temperature for the BWR/4 model.

BWR/2

A single-case sensitivity of PCT history to ECCS temperature for a BWR/2 0.25 ft^2 small break scenario is presented in Figure 8.3-15 of the LTR. [[

]]

It is necessary, however, to assess the influence of ECCS temperature on the limiting BWR/2 break scenario, where the PCT is indeed high enough to warrant examination of the sensitivity of maximum oxidation thickness. This sensitivity is evaluated using [[

]] described above for BWR/4. [[

]]

The PCT sensitivity results presented in Table R30-2 show [[

]]. The maximum oxidation thickness results presented in Table R30-3 show [[

]]

Given the sensitivity described above, the nominal ECCS temperature of [[ ]] is a reasonable best-estimate condition for BWR/2 calculations.

Table R30-1 BWR/4 PCT Sensitivity to ECCS Temperature

[[		
		]]

Table R30-2 BWR/2 PCT Sensitivity to ECCS Temperature

[[		
		]]

Table R30-3 BWR/2 Oxidation Sensitivity to ECCS Temperature

[[		
		]]

LTR Impact

No changes to the LTR are proposed as the result of this RAI response.

RAI-31

31) Please explain further why it is not necessary or desirable to include biases in the break spectrum calculation (section 8.1.6). It is not clear that excluding biases would provide an acceptable method for identifying the limiting break location (discharge and suction breaks are observed to result in similar PCTs for both BWR/4 and BWR/6 demonstration cases) and size range that is potentially limiting for performing statistical calculations.

RAI-31 Response

The break spectrum analyses for LOCA application, such as presented in LTR Section 8.1.5 for BWR/4, are a screening tool used for determining the vicinity of the limiting break and the PCTs from these runs do not directly enter to the downstream runs. The break spectrum profile for a particular plant is mainly dependent on the ECC system. Among the major parameters affecting the limiting break size are available systems per single failure assumption, amount of available coolant delivered based on ECCS performance, and system setpoints. The model biases are not expected to change the limiting break size significantly. This can be demonstrated by comparing the curve labeled "Nominal" in LTR Figure 8.1-29 (with model biases removed) to the curves in LTR Figure 8.1-23 (with model biases included). From the determination of the limiting break size point of view, those curves are comparable, both of which effectively determine the vicinity of the limiting break for this plant type. This is also true for other BWR types, as shown in LTR.

The analyses support the conclusion that including or not including the model biases in the break spectrum analysis has insignificant impact in determining the limiting break scenario and size for each plant type. This conclusion is further confirmed by the analyses using the detailed core model (see the response to RAI-6 for the description of the detailed core model). Figure R31-1 shows the comparisons of the break spectrums obtained at different conditions for BWR/4 (As an example, only the break spectrum for suction break is shown here. Similar results are obtained for the discharge break). The curve labeled "LTR Core (Figure 8.1-23) – Biased" is the same curve from LTR Figure 8.1-23. For this curve, model biases are included. The other two break spectrum curves are both obtained with the detailed core model. The difference between these two curves is that one is obtained with model biases included (biased) and the other one with model biases removed (non-biased). [[

]] In the LTR, no particular position was declared for this aspect of the break spectrum as 'not necessary' or 'desirable'.

For TRACG LOCA application, the overall analysis approach is further explained in Chapter 9. The break spectrum is traditionally determined from best-estimate nominal results. The limiting break size from the nominal break spectrum is analyzed by applying the uncertainty parameters to determine the upper tolerance results. In addition to the limiting break size identified in the nominal break spectrum, at least two other break sizes will be analyzed in the statistical evaluation to ensure that the uncertainties associated with the analysis are adequately quantified.

LTR Impact

No changes to the LTR are proposed as the result of this RAI response.

[[

]]

Figure R31-1 BWR/4 Break Spectrum for Recirculation Line Suction Breaks with Battery failure.

(DE GB: Double-Ended Guillotine Break; Biased: model biases included;

Non-biased: model biases removed)

RAI-32

32) The loss of an isolation condenser is taken as the limiting failure for the BWR/2 demonstration calculations in section 8.3.2.1. Given the marginal impact expected for the isolation condenser in mitigating a large-break LOCA, the basis for this choice is not clear. Although the TR states that the demonstration case core spray system is single-failure proof, these systems may experience failures (e.g., a booster pump or redundant pump) that degrade the system flow rate and/or discharge pressure. As such, it appears likely that the operational status of components within the core spray system may influence PCT and oxidation more than the isolation condensers. Please demonstrate the sensitivity of the BWR/2 to postulated single failures within the core spray system to identify whether these failures may be more limiting than the demonstration case. Based on the evaluation model proposed in the TR, the net influence of core spray system subcomponents is not clear due to the competing effects of increased spray cooling and the degradation of condensation heat transfer due to infiltration of noncondensible gases.

RAI-32 Response

It is necessary to correct a misunderstanding that was caused by the wording used in Section 8.3.2.1.

ECCS configuration for a typical BWR/2 is shown in Figure R32-1. In performing the ECCS performance analysis the postulated failure of a single active component will never result in less than certain minimum combinations of remaining operable systems.

For an assumed single failure of an Isolation Condenser (IC), it is conservatively assumed that the unfailed ICs are connected to the broken recirculation loop so that no ICs remain available. This single failure assumption is bounded by never crediting the ICs regardless of what other single failures are postulated. This approach supports the NRC premise that the ICs which have no ability to make up lost inventory have minimal impact in mitigating a large break LOCA.

For the scenario where the assumed single failure is one of the diesel generators, at least 2 Core Spray trains (2 sets of CS pump and booster pump) will remain available out of 4 CS trains shown in Figure R32-1. Any other single failure related to the CS pump, booster pump, CS lines, or sparger would still result in a minimum of two functional 2 CS trains (hence the analyzed minimum configuration crediting 2 CS trains is described as “single failure proof”). Assuming an additional booster pump failure (unless requested by customer for operational purposes) on top of the already assumed single failure makes the analyzed scenario beyond design basis because the scenario requires multiple failures. An example of a beyond-design-basis multiple failure scenario is DG failure (which takes 2 CS trains out) plus failure of a booster pump in one of the two remaining available CS trains.

The analyzed scenarios for the BWR/2 demonstration calculations adequately address the single failure requirements by crediting only the minimum configuration of two operational CS trains.

LTR Impact

No changes to the LTR are proposed as the result of this RAI response.

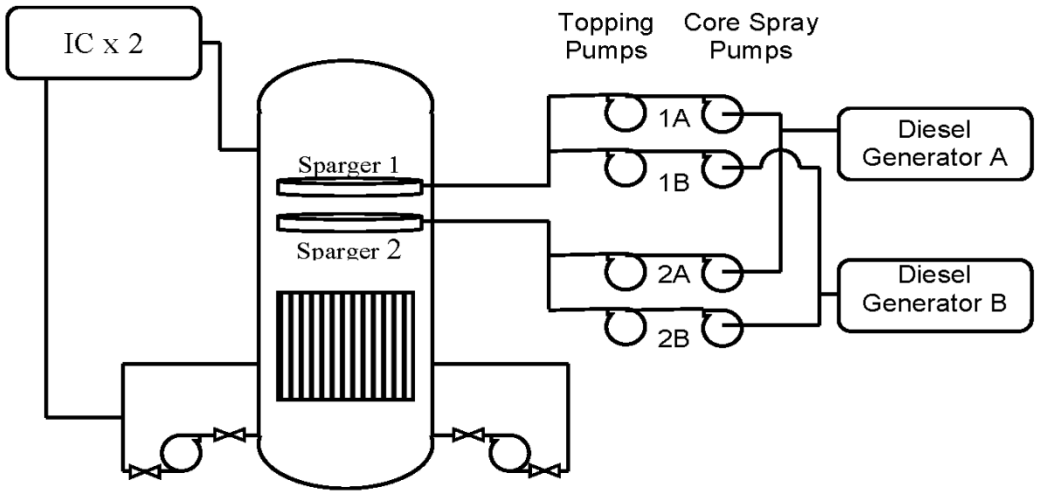

Figure R32-1 A Typical BWR/2 ECCS Configuration

RAI-33

33) Please provide the following information related to PIRT item C18 (cladding perforation):

a. A summary of or reference for the tests that includes the number of tests, the type(s) of cladding tested, and the heatup rates used.

b. The basis for applying the empirical data used to estimate clad rupture stresses to current-generation fuels.

c. The basis for the assumption of normality for the upper and lower 95 percent groups used to determine the rupture stress.

d. Explanation of the origin of and justification for the assumed uncertainty of the built-in fuel rod internal pressure curves and the normality of the multiplier on rod pressure.

e. Relative to the high-temperature phase change of zirconium, please clarify the statement on page 2-11 of the TR that phase change of in-core materials is not modeled.

RAI-33 Response

a. A summary of the cladding hoop stress versus perforation temperature testing used in defining the model and model uncertainty can be found in Reference R33-1. The figures in the referenced letter's enclosed report shows the comparison of high temperature test data to the rupture stress model. All of the tests presented are performed for heat-up rates [[

]]. The following symbol key gives the types of cladding tested, as presented in Figure 5.

[[

]]

b. The clad rupture stress model is assessed using hoop stresses, as described by the method in Section 3.1 of Reference R33-2. By employing this method of converting differential pressure data to hoop stress data, design-specific dimensional effects are eliminated. This allows the clad rupture stress model to be extended beyond the 7x7 and 8x8 fuel from the test programs to current-generation fuel product lines. Additionally, the data in Reference R33-1 show that the differences between 7x7 and 8x8 fuel rods are insignificant compared to the scatter in the data, confirming that dimensional effects have been eliminated.

c. The clad rupture stress uncertainty model was developed using temperature-dependent rupture stress data from GE material testing programs. The uncertainty model directly uses temperature-dependent summary data from these testing programs, including average rupture stress and the upper and lower bounds for 95% of the data. At each temperature, two half-normal distributions are used to construct a representation of the rupture stress distribution at that temperature. An example of this process is shown in Figure R33-1. In this application, the use of half-normal distributions is a simplification

to allow for the construction of temperature-dependent continuous probability distributions. While the half-normal distributions are used in the absence of normality tests of the model to data, they are preferred over uniform distributions, because normal distributions allow for the possibility of conservatively producing sampled values beyond the 95%-confidence interval.

d. The LHGR- and exposure-dependent values of fuel rod internal pressure uncertainty used in TRACG LOCA analyses are calculated based on fission gas release using combination of uncertainties evaluations. These evaluations, performed at [[

]]

The actual uncertainty values for rod internal pressure applied in the LTR demonstration models are also presented in LTR Figure 5.1-16, where the model values are shown to [[

]] Treatment of the uncertainty multiplier on rod pressure as belonging to a normal population does not imply that the uncertainty population of this parameter is indeed normal. In this case, the normal distribution is a tool used to provide complete coverage of the possible values of rod internal pressure prior to the transient.

It is noted that the data presented in LTR Figure 5.1-16 represents rod internal pressure uncertainties from GESTR thermal-mechanical analyses. This calculation method has been qualified previously (Reference R33-3). The exposure-dependent uncertainties used in any TRACG LOCA plant application will be calculated using PRIME thermal-mechanical analyses (qualified in Reference R33-4) specific to the appropriate plant-type and fuel product line. It is largely understood, however, that the key driver of rod perforation is the temperature-dependent rupture stress. The rod internal pressure may alter slightly the timing of perforations but would ultimately have minimal effect on the amount of equivalent cladding reacted.

e. On page 2-11 of the TR, GEH indicates the following:

> TRACG does not model physical and chemical changes in in-core materials. These phenomena are not significant for BWR LOCA.

Rod internal pressure and the resulting hoop stress are modeled in TRACG for the purpose of tracking geometric changes due to rod perforation and to account for the resulting oxidation of the cladding. Additionally, material properties for the cladding and fuel take into account transient temperature effects. Physical and chemical changes resulting from cladding temperature transients, however, are not modeled. If the 10 CFR 50.46(b) acceptance criteria for ECCS systems are met, the effects of eutectic formation and phase change have no adverse impact on the fuel and can be ignored in cladding response calculations within the range of post-LOCA conditions.

[[

]]

Figure R33-1 Example of Half-Normal Distribution Generation Based on Experimental Data

References

R33-1. Letter from R. W. Bucholz (GE) to C. S. Rubenstein (NRC), "General Electric Fuel Clad Swelling and Rupture Model," May 15, 1981, MFN-097-81.

R33-2. NUREG-0630 Cladding Swelling and Rupture Models for LOCA Analysis, April 1980.

R33-3. B.S. Shiralkar, et al. "The GESTR-LOCA and SAFER Models for the Evaluation of the Loss-of-Coolant Accident, Volume I: GESTR-LOCA – A Model for the Prediction of Fuel Rod Thermal Performance," NEDE-23785-1-PA, Revision 1, October 1984.

R33-4. "The PRIME Model for Analysis of Fuel Rod Thermal-Mechanical Performance Part 3 – Application Methodology," NEDC-33258P, Revision 1, September 2010.

LTR Impact

The following changes to LTR Section 5.1.3.24 will be made.

5.1.3.24 C18 – Fuel Cladding Strain /Perforation (H)

The TRACG parameters governing strain-induced fuel rod perforation are the clad rupture stress and the rod internal pressure. Based on material properties, the rupture stress and its associated uncertainty is modeled in TRACG as three curves corresponding to best-estimate, lower 95%, and upper 95% rupture stress curves as functions of cladding temperature (Figure 5.1 15). At each temperature, the upper and lower 95% bounds are used to define half-normal PDFs above and below the best-estimate rupture stress, respectively. This is done on the basis that the upper and lower 95% points are removed by 1.645σ from the best-estimate value.

The instantaneous clad hoop stress is directly related to the fuel rod internal pressure. The uncertainty in fuel rod internal pressure, which is dominated by the uncertainty in fission gas release, is expressed as a function of peak pellet exposure and linear heat generation rate (LHGR)**. The uncertainty in fission gas, and therefore fuel rod internal pressure, is calculated in a fuel-dependent analysis that combines the uncertainties in coolant pressure, pellet composition, and rod geometry. A qualified and approved model [24, 76] is used for performing such analyses. An example of the thermal-mechanical analysis results for the uncertainty in fuel rod internal pressure as used in the Chapter 8 demonstration analyses is** ~~as~~ shown in Figure 5.1-16. **In support of a TRACG LOCA plant application, a fission gas uncertainty calculation specific to the appropriate plant-type and relevant fuel product line will be used to sample the rod internal pressure values.** The open and closed symbols in Figure 5.1-16 denote, respectively, the pressure uncertainty for fuel with 7% gadolinium and fuel without gadolinium. The curves shown by solid lines have been built into TRACG to represent the uncertainties for both gadolinium and non-gadolinium fuel. The built-in curves are extrapolated back to a [[

]]

RAI-34

34) From the discussion of PIRT entry B9 (three-dimensional effects of LPCI injection into the bypass region) in section 5.1.2.9, the basis for disposition of the issue appears to reference a nodalization sensitivity study performed for a BWR/4, for which the effect is presumably not relevant. Please provide adequate basis that increased azimuthal nodalization of the vessel is not necessary for modeling a BWR with LPCI injection into the bypass region, discussing any sensitivity studies that have been performed specifically for this case.

RAI-34 Response

This RAI is only applicable to the plants with LPCI injection to the core bypass region, such as BWR/5 and BWR/6. It is understood that the mixing of the LPCI with the bypass liquid may result in non-uniform liquid temperatures at the bottom of the bypass, and eventually at the bottom of the fuel bundles. As shown in the demonstration calculations in LTR Section 8.2, LPCS is more effective than the LPCI in preventing excessive cladding temperature heatup. Therefore it is expected the impact of non-uniformity of the LPCI mixing with the fluid in the bypass region on the peak cladding temperature is not significant, and the increased azimuthal nodalization of the vessel is not necessary.

To demonstrate that increased azimuthal nodalization of the vessel is not necessary for modeling a BWR with LPCI injection into the bypass region, sensitivity study was performed with the BWR/6 limiting break case (discharge break size of 0.093 m^2 with HPCSDG failure) using the same nodalization described in LTR Figure 8.2-1.

In this sensitivity study,
[[ ]] as shown
in Table R34-1. Changing the
[[
]]

Table R34-1 LPCI Parametric Study Cases

Case	LPCI Condition	Differences from Nominal (K)
1	[[	
2		
3		
4		
5		
6		
7		
8		
9		]]

The difference in PCT for the sensitivity cases are reported in Table R34-1 and it can be seen that [[

]]

The fuel cladding temperatures of the PCT bundle, in addition to the nominal LPCS and LPCI flow rates, are depicted in Figure R34-1. It shows that [[

]]

Based on the results of this BWR/6 LPCI sensitivity, it is concluded that increased azimuthal nodalization of the vessel is not necessary for modeling a BWR with LPCI injection into the bypass region.

LTR Impact

No changes to the LTR are proposed as the result of this RAI response.

[[

]]

Figure R34-1 BWR/6 LPCI Sensitivity Studies: Clad Temperatures and ECC Flow Rates

RAI-35

35) Unlike the other BWR demonstration calculations, the boiling transition peak for the BWR/2 case is not fully quenched for the limiting channel/rod. Thus, the temperature increase associated with boiling transition contributes to the eventual PCT. As such, please provide further justification that parameters affecting the boiling transition temperature increase (e.g., void coefficient, Doppler coefficient) do not appreciably influence the ultimate PCT.

RAI-35 Response

For LOCA applications, the flow component of the power/flow mismatch drives the early boiling transition (BT). In large break LOCAs, voiding in the core due to rapid pressure reduction is sufficient to reduce fission power to almost zero even before the scram becomes effective. Small variations in fission power are not important because the heatup is mainly caused by lack of coolant. During a LOCA transient, the core power drops down to decay heat levels within seconds following the scram. Only for small breaks where the scram may be delayed is the void coefficient and its uncertainty of minor importance. See LTR Sections 5.1.3.1 and 5.1.3.2 for a description of the void coefficient modeling and its impact on fission power. In general, fission power is a very small fraction of the time-integrated total power and any uncertainty in void or temperature reactivity coefficients has an insignificant effect on the thermal response of the fuel. The most important uncertainties with respect to determining the PCT are those associated with decay heat, stored energy in the fuel, and post-BT heat transfer.

LTR Impact

No changes to the LTR are proposed as the result of this RAI response.

RAI-36

36) PIRT item C3 includes phenomena associated with dynamic gap conductance and gap size, mainly focusing on post-scram pellet contraction. Please clarify whether the impact of clad ballooning on gap size is captured in this or another PIRT item, and explain how the assigned uncertainty derived from pellet conductivity applies to or bounds the effect of clad ballooning. Please further characterize the approximate lower temperature threshold at which GEH considers ballooning important and identify whether the BWR/2 small-break LOCA, for which PIRT item C3 is ranked low, could reach this range.

RAI-36 Response

PIRT C3 is only one of the parameters that is relevant to ballooning. Uncertainty in the pressure of gases in the gap addressed by C18 is actually more relevant to ballooning. See also the discussion for PIRT C18 in the LTR (NEDE-33005P) and the response to RAI-33.

The dynamic gap model is described in Section 7.5.2 of LTR reference [1] (TRACG Model Description, NEDE-32176P, Revision 4). The discussion for C3 in the LOCA Application LTR (NEDE-33005P) pertains primarily to gap conductance which deals with both the size of the gap and the conductivity of gases in the gap. [[

]]

The uncertainties in gap conductance and gap size address only the phenomena for conditions when the gap is open or at least partially open. The discussion for PIRT item C3 focuses on the dynamic thermal contraction of the fuel pellet following the scram because the conditions where the fuel pellet has contracted away from the cladding inner surface result in a lower effective heat transfer coefficient between pellet and cladding than the case where the gap is closed. This lower overall heat transfer coefficient has a minor impact on the stored energy retained in the fuel pellet during the early stages of a LOCA. Whether the gap is open or closed, the dominant heat transfer resistance is the thermal conductivity of the fuel pellet which is why it is treated using C3BX. Note that the importance of both pellet thermal conductivity and gap conductance uncertainties decrease during the LOCA as the power drops to decay heat levels after the scram resulting in a greatly reduced heat flux from the fuel rod.

When the gap is completely closed, the pellet is in contact with the cladding and the primary stress associated with this condition is pellet and cladding contact pressure. [[

]]

Dynamic gap modeling applies to both opening and closing of the gap. When the gap is open the pellet retains more decay heat energy which causes the pellet to heat up and expand toward the gap. The contraction and expansion rates for the pellet and cladding are different which changes the gap size and feeds back into the pellet-cladding heat transfer. The strain rates for the pellet and cladding are also different and both depend on their respective temperatures. For higher temperatures and higher internal gas pressures, the clad can expand outward faster than the fuel pellet, thus resulting in ballooning. For this phenomenon [[

]]

For an open gap the primary radial stress is caused by the difference between the internal gas pressure and the fluid pressure outside the cladding. [[

]] Uncertainty for the internal gas pressure is accounted for by PIRT C18 [[ ]] as discussed further in the response to RAI-33. The gap size is an important feedback mechanism. The dynamics for how the pellet size changes depends on the fuel temperature and changes in the pellet size feeds back into the volume available for gases inside the cladding thus affecting the internal gas pressure. [[

]]

Clad ballooning and cladding perforation are closely related because both are determined by the relationship between cladding stress and strain. The fuel rod cladding perforation model is described in Section 7.5.3.3 of LTR reference [1]. [[

]] There are many uncertainties of high importance in the LTR that address the ability to calculate cladding temperatures. As described in Section 7.5.3.3 of LTR reference [1], [[

]]

Variable gap conductance (C3) is ranked [[

]] The critical parameter of interest is peak clad temperature (PCT). As explained above, C3 influences the initial conditions [[

]] For the BWR/2 in particular, the break size of most concern is the DBA large break because of the inability to refill the vessel and reflood the core which results in higher calculated peak clad temperatures (PCTs). In any event,

the highest importance ranking overall for C3 is [[

]]

The uncertainty attributed to lower fill gas pressures for BWR/2 fuel is addressed [[

]] For uncertainties affected by C18, the primary critical parameter of concern is oxidation because once the cladding perforates the inside of the cladding can start oxidizing and effectively double the local oxidation rate.

LTR Impact

No changes to the LTR are proposed as the result of this RAI response.

RAI-37

37) In Table 3.4-1, PIRT entry F3 indicates that the PCT transient is over before the vessel is depressurized to containment pressure. However, this does not appear consistent with Figures 3.2-6 (showing nearly complete depressurization by approximately 100 seconds) and 3.2-9, as well as independent calculations performed by the NRC staff. Therefore, please either clarify the technical basis or revise the statement.

RAI-37 Response

It is acknowledged that the sentences in Table 3.4-1 stating the "PCT transient is over before vessel is depressurized to containment pressure" are not completely true, especially for BWR/2 transients. Moreover, these sentences do not add any value for the discussion and have no impact on the demonstration calculations.

The sentences stating the "PCT transient is over before vessel is depressurized to containment pressure" will be deleted in the LTR revision of Table 3.4-1 for PIRT items F3 and M3.

LTR Impact

The sentence in Table 3.4-1 will be deleted in two places as discussed above.

RAI-38

38) PIRT item M3 is ranked medium, even for the BWR/2 case. However, based on the demonstration calculations, M3 appears to have a dominant impact on the PCT. Please clarify whether GEH considers the PIRT to be fundamentally correct (i.e., the influence of this factor in code simulations is primarily due to a conservative assumption regarding the containment boundary condition), or whether an increased ranking should be assigned for the BWR/2 case.

RAI-38 Response

The results in the LTR have shown that PIRT item M3 (or F3) [[

]]

LTR Impact

No changes to the LTR are proposed as the result of this RAI response.

RAI-39

39) Sections 4.3.3.2 and 4.3.3.1 referred to in the component performance qualification column of Table 4.2-1 do not appear to exist in NEDE-32177P, Revision 3. Please clarify whether these section numbers refer to NEDC-32725P, which addresses passive systems of the Simplified Boiling Water Reactor. Please explain the relevance of this testing to operating reactors or remove these references from NEDE-33005P.

RAI-39 Response

These section numbers were erroneously retained from an early draft of NEDE-33005P. The section references are to a planned revision of NEDE-32177P that was subsequently cancelled. Section 4.3.3.1 intended to refer to SSTF Upper Plenum testing, which is now Section 4.3 in Revision 3 of NEDE-32177P. Section 4.3.3.2 was intended to refer to SSTF Lower Plenum testing. SSTF Lower Plenum test is not explicitly discussed in Revision 3 of NEDE-32177P but some of the comparisons between the TRACG04 calculations and the lower plenum data are contained in Section 5.3 in Revision 3 of NEDE-32177P.

It should be noted that there are other references in Table 4.2-1 that are also not in Revision 3 of NEDE-32177P. In particular, 4.5, “PANTHERS”, is in NEDE-32725P Section 4.2. Section references to 4.1.4, “Two-Phase Jet Pump”, and 4.6, “Channel Leakage Flow” are not in either document.

LTR Table 4.2-1 will be revised to be consistent with Revision 3 of NEDE-32177P.

LTR Impact

Table 4.2-1 in the LTR will be revised as described above.

RAI-40

40) Regarding PIRT items C2AX, B2, and C23, please justify that random perturbations to the distribution parameter (C_0 - 1) and entrainment coefficient (η) are sufficient to provide the expected variation in void distribution, addressing the specific issues below:

a. Based on a comparison of Figures 5.1-8 and 5.1-9 to Figure 5.1-17, it is not clear that [[

]] Similar limitations in reproducing the deviations in [[

]] as well.

b. Please justify that [[

]] in a simplified geometry for different flow regimes (i.e., bubbly/churn, transition, annular) may help to demonstrate adequacy.

c. Although GEH noted desirable properties of the [[

]] and justify that the distortion is either negligible or conservative.

d. Please compare the range of mass fluxes used in the Toshiba tests (section 5.1.3.3) with the mass fluxes expected for the hot bundles under limiting LOCA conditions and justify that the difference does not impact the assumed uncertainty distribution.

RAI-40 Response

This RAI has stimulated a reexamination of the process for covering the Toshiba void experimental data within the TRACG calculations. This response will first directly answer the questions listed above and will secondly describe the latest analysis basis that ultimately concludes [[

]].

a. There is merit to the observation that [[

]]

b. [[ ]] is no longer an issue with [[ ]].

c. As indicated in the response to part b., [[ ]]. The probability density function in Figure 5.1-10 is incorrect and will be replaced as the result of this RAI.

d. The mass fluxes from the Toshiba test database are [[ ]] These are similar to the observed mass fluxes in the hot channels of the demonstration BWR/4 model during the time of interest. Here, the time of interest is defined as the point in the transient where the system pressure reaches the low-pressure test condition from the Toshiba experiments. This time is approximately concurrent with the inventory recovery in the channel and the peak PCT. This confirms that the Toshiba database is appropriate to supplement the qualification of TRACG void calculations at low pressure conditions during the vessel blowdown.

As mentioned above, GEH has performed extensive design work to strengthen the basis for predicting void fraction in low-pressure conditions for LOCA calculations. These activities were manifold and included increasing the database of void fraction comparisons from additional Toshiba tests, [[

]]

The previous work included only [[ ]] tests from the available Toshiba void fraction data for TRACG comparisons. Of these, [[ ]] tests were conditions where high void fractions were predicted. To enhance the understanding of low-pressure void calculation resolution compared to experiment, an additional [[ ]] test points from the Toshiba data were modeled in TRACG, expanding the full database to [[ ]] tests, [[ ]]. The original [[ ]] tests were conducted with [[

]]. The full database is for the same pressure and flows, but also uses [[

]]. TRACG predicted the expanded Toshiba data with a bias of [[ ]] and a standard deviation of [[ ]]. Figure R40-1 indicates that it is reasonable to assume that the void fraction devations are normally distributed.

In an effort to justify [[

]], each of the points in the expanded Toshiba database was studied using [[

]]

The statistical evaluations on the expanded Toshiba database also included [[

]]

The results from this study are presented in Table R40-1, where it is shown that the Toshiba data error has [[

]]. This uncertainty is [[ ]] when only the high void cases are considered, which is the region of interest for hot channel modeling in post-LOCA conditions.

[[

]] The expanded study discussed here proved [[

]]. Expanding the database from [[ ]] to [[ ]] samples in this study gave even higher confidence in that conclusion. Considering the lessons learned from these evaluations, [[

]].

Table R40-1 Numerical Summary of Toshiba Void Test Evaluations

[[			
			]]

[[

]]

Figure R40-1 Void Fraction Deviations for Expanded Database of Toshiba Tests

[[

]]

Figure R40-2 Graphical Summary of Toshiba Void Test Evaluations with [[
]]

LTR Impact

Section 5.1.3.3 will be rewritten as the result of this RAI response. Additionally, Figure 5.1-10 will be replaced by Figure R40-3.

[[

]]

Figure R40-3 Lognormal Probability Distribution for PIRT22

RAI-41

41) In section 5.1.1.9, the TR references NEDE-32177P, Revision 3, as containing a study of increasing the azimuthal sectors in the vessel from [[ ]] However, the NRC staff only located discussion of sensitivity studies that varied the number of azimuthal sectors from [[ ]] (Table 6.9-2 of NEDE-32177P, Revision 3, and Table 5.2-1 of NEDE-33005P). Please clarify whether additional sensitivity studies have been performed for azimuthal nodalization of the vessel and provide the results.

RAI-41 Response

A BWR/4 [[ ]] model was utilized in a 2002 nodalization sensitivity study for TRACG LOCA. The model consisted of [[

]]

This sensitivity study was not documented in the Qualification LTR. Thus, the TRACG LOCA LTR should not reference the Qualification LTR regarding the six-sector sensitivity study.

LTR Impact

Reference [2] will be removed from Section 5.1.1.9 of the LTR as shown below.

5.1.1.9 A11 – 3-D Effects (M)

Modeling of the lower plenum must also address possible azimuthal variations in the thermodynamic variables that may influence the plant response to a LOCA. A nodalization study ~~[2]~~ was performed to ensure that the effects of azimuthal variations were adequately represented in the TRACG plant models. Increasing the number of azimuthal sectors from one (standard model) to [[ ]] for the BWR/4 design basis accident (DBA). The one-sector model can be used for the TRACG LOCA calculations because the modeling simplicity thereby realized [[ ]] that would result from the use of a more refined model.

RAI-42

42) Please clarify the basis for the [[
]] From the references cited in section 5.1.3.6, the justification for the individual uncertainties and their combination (i.e., presumably square root sum of squares) was not clear to the NRC staff.

RAI-42 Response

As discussed in the LTR, the TRACG fuel rod model based originally on the GESTR model has been updated to incorporate fuel thermal conductivity from PRIME (See the response to RAI-24). According to References [3] and [66] of the LTR, the overall uncertainty in pellet heat transfer is [[
]] and valid for PRIME (Reference [76] of LTR – NEDC-33258P-A, Revision 1).

For TRACG LOCA applications, two additional uncertainties in Reference [76] of the LTR are included to account for the transient variation. These two additional uncertainties are:

[[

]]

Therefore the total overall uncertainty [[
]], and is used for the LTR demonstration calculations.

LTR Impact

No changes to the LTR are proposed as the result of this RAI response.

RAI-43

43) Please clarify the statement in section 5.1.3.10 that an uncertainty of [[ ]] is sufficient to bound the uncertainty in the side entry orifice (SEO) loss coefficient. Specifically, please identify the source of the available data and the extent to which it is applicable to two-phase flow conditions during a LOCA.

RAI-43 Response

Pressure drops at various locations, including SEO and Lower Tie Plate (LTP) for the 9x9 and 10x10 fuel bundles, were measured and the results can be found in Reference R43-1 and R43-2, respectively. The measurements were performed with single phase water inlet conditions. The uncertainty in pressure drop for the 9x9 and 10x10 SEO and LTP are documented in Table 5.1-1 of the TRACG Application for ESBWR Stability Analysis (Reference R43-3).

The two-phase pressure drop at the SEO is calculated in TRACG using the homogeneous two-phase multiplier. The uncertainty in the two-phase multiplier is estimated in Section 6.2.2.5 of NEDE-32176P, Rev. 4 to range from [[ ]]. For other TRACG applications (References R43-3 and R43-4), a [[ ]] uncertainty has been conservatively assumed in the SEO loss coefficient for single phase conditions. For LOCA application, a [[ ]] is applied to bound the RMS of the single-phase and two-phase uncertainty components. For two-phase conditions typical of a BWR LOCA, there are numerous comparisons against integral system data that confirm the accuracy of the modeling of the two-phase losses as indicated in Section 6.2.3 of NEDE-32176P, Rev. 4. Relevant comparisons between TRACG calculations and the test data are made for TLTA, FIST, GIST, and others in the TRACG Qualification LTR, NEDE-32177P, Rev. 3.

References

R43-1 NEDC-31491P, “Retrofit Lattice Component Pressure Drop Tests for the STEP II Fuel Design Standardization Program,” November 1987.

R43-2 NEDC-31998P, “STEP III Lower Tie Plate Pressure Drop Test with the BWR/2-5 Channel,” December 1991.

R43-3 NEDE-33083 Supplement 1P, Revision 2, “TRACG Application for ESBWR Stability Analysis,” September 2010.

R43-4 NEDE-33147P-A, Revision 4, “DSS-CD TRACG Application,” August 2013.

LTR Impact

No changes to the LTR are proposed as the result of this RAI response.

RAI-44

44) With reference to section 5.1.3.19, please clarify whether fuel-specific biases and uncertainties will be used in conjunction with the GEXL correlation, as in NEDE-32906P, unless acceptable statistical analysis demonstrates that data for different fuel types may be pooled.

RAI-44 Response

As explained in Section 5.1.3.19, either fuel-type specific values for the GEXL bias and uncertainty will be applied or a more conservative GEXL bias and bounding uncertainty that bounds all fuel types in the core will be applied. GEXL uncertainty and biases can be applied in the TRACG code on a CHAN group basis. A more conservative bounding approach will be applied for competitor fuel designs where determining the precise values is more difficult.

LTR Impact

No changes to the LTR are proposed as the result of this RAI response.

RAI-45

45) Please provide additional technical basis for the assumption that the uncertainty distribution for the Sun-Gonzalez-Tien correlation is [[
]]. Intuitively, the additional degree of freedom (i.e., droplets) implies the potential for greater uncertainty relative to a single-phase correlation. Please clarify whether adequate experimental data exists to estimate the uncertainty specific to the Sun-Gonzalez-Tien correlation. Please further justify the adequacy of the assumed uncertainty distributions in the large region ($0.1<\alpha<0.5$) in which the Sun-Gonzalez-Tien and Bromley correlations are interpolated.

RAI-45 Response

There are no known experimental data that could be used to estimate the uncertainty in the Sun-Gonzalez-Tien correlation. Consequently, the basis for the assumed uncertainties is engineering judgment. Note that perturbations are concurrently imposed that account for uncertainties in the void fraction. This will cause an additional perturbation in the applied heat transfer coefficients. The confirmation of the reasonableness of this choice is demonstrated by the statistical analyses for the integrated tests, especially the Core Spray Heat Transfer (CSHT), as presented in the LTR Section 7. With the proposed model uncertainties in LTR Section 5, the test data are well covered by the TRACG predictions.

For TRACG film boiling heat transfer calculations, it should be clarified that Sun-Gonzalez-Tien correlation is not used for the low void flow region (void fraction of 0.1 to 0.5 region); rather it is only used in high void fraction region (dispersed flow regime), and in the transition region from the inverted annular flow to the dispersed flow, where both Bromley and Sun-Gonzalez-Tien correlations are used with a weighting factor depending on the void fraction. See the discussion in Section 6.6.10.2 of NEDE-32176P, R4. For even lower void fractions, the modified Bromley correlation is used. See the discussion in Section 6.6.9.2 of NEDE-32176P, R4 for details on TRACG implementation.

LTR Impact

No changes to the LTR are proposed as the result of this RAI response.

RAI-46

46) Please confirm whether the data that is the basis for the uncertainty distribution for PIRT item C16 is the data shown in Figure 6-33 of NEDE-32176P, Revision 4. Please further justify the adequacy of the proposed uncertainty range given the limited size of the database.

RAI-46 Response

Data shown in Figure 6-33 of NEDE-32176P, Rev. 4 is the basis used to bound the uncertainty range of [[ ]] variation in thermal emissivity. For these steady-state tests, no liquid was injected at the top of the fuel bundle and the bundle contained only stagnant air. Under these conditions, the convective heat transfer is minimized and radiation heat transfer is the dominant mode. Core Spray Heat Transfer (CSHT) tests have been used for this qualification, as discussed in Section 6.6.10.3 of NEDE-32176P, Rev. 4. Note that [[
]] The limited amount of data to establish this component of the overall uncertainty in heat transfer is justified because for LOCA calculations the contribution due to thermal radiation is not dominant. The overall applicability and uncertainty associated with PCT calculations is justified by comparisons to data provided from the CSHT, THTF, TLTA, FIST, ROSA-III, FIX-II and GIST tests as documented in NEDE-32177P, Rev. 3.

LTR Impact

No changes to the LTR are proposed as the result of this RAI response.

RAI-47

47) Please address the following issues associated with the discussion in section 5.1.3.23:

a. Heat transfer references indicate that the Dittus-Boelter correlation is appropriate for small to moderate temperature differences. The correlation tends to overpredict heat transfer at large temperature differences because it does not account for variations in physical properties due to the temperature gradient at a given cross section. The NRC staff understands that temperature differences of approximately 200-300K (jet-pump BWRs) and 400-600K (non-jet-pump BWRs) or higher can exist between fuel rods and steam during a LOCA. However, based on the results presented in NEDE-13462, the tests appear to be based on temperature differences of approximately [[ ]] Please clarify whether allowance is made for the effect of the temperature difference in deriving the uncertainty distribution parameters and provide justification.

b. Please justify that no significant scaling issues arise from applying biases and uncertainties associated with tests using a [[ ]] bundle to a full-sized bundle. For example, please explain why the [[ ]] bundle tested would not underpredict the temperature for the interior rods of a full-size bundle based on an underestimation of edge-to-center variation and an overestimation of mixing and heat transfer to peripheral rods and the channel wall. Has subchannel analysis been performed to validate that scaling effects are insignificant?

c. The basis for the [[ ]] for internal rods appears to be derived from a deviation calculated from a bundle-averaged approach for the [[ ]] test bundle (i.e., including heat transfer from both interior and peripheral rods). Therefore, if a bias is applied only to heat transferred from interior rods, please clarify why the requisite bias would not need to be scaled up proportionally.

RAI-47 Response

a. No allowance was made for the effect of the temperature difference in deriving the uncertainty distribution parameters in the LTR Section 5.1.3.23. The uncertainties in Section 5.1.3.23 are based on the test data in NEDE-13462, June 1976. However, the impact of the variations in fluid physical properties due to high temperature difference between the wall and vapor on the prediction of Dittus-Boelter correlation for vapor heat transfer is considered in TRACG code, as discussed in Section 6.6.5 of NEDE-32176P, R4, January 2008. The heat transfer coefficient for single phase steam flow is calculated using Dittus-Boelter correlation when the flow is in the turbulent regime. When wall temperature (Tw) is greater than the vapor temperature (Tv), the heat transfer coefficient predicted by Dittus-Boelter is multiplied by a factor (Tv/Tw)^0.5 to account for the increased vapor temperature.

b. The current steam cooling uncertainty adopted in the LTR is derived based on the [[

]]This indirectly demonstrated that the scaling impact is not significant.

c. As discussed in Section 5.1.3.23 of the LTR, the bias of [[ ]] for the Dittus-Boelter heat transfer coefficient for internal rods are derived from two sources: [[

]] in NEDE-13462. The conversion factor is, however, based on 60 bundle internal rod measurement points presented in NEDE-13462.

For the demonstration calculations in the LTR, the bias developed for this PIRT is only applied to the internal rods in the bundles. However, it does not have to be scaled up. As discussed at the end of Section 5.1.3.23 and Figure 5.1-14 in the LTR, the bias from 60 internal rod measurement points presented in NEDE-13462 is estimated as [[ ]] based on all measure points in NEDE-13462. This slightly smaller prediction bias for the internal rods was expected because the internal rods are impacted less by the channel wall boundary than the external rods.

LTR Impact

It is suggested that the following two sentences in Section 5.1.3.23 of the LTR

> The data described in Reference [56] include 1935 measurement points. Of these, 60 points from four runs are shown graphically in the report along with the steam temperature calculated by both the bundle average and extended rod-centered subchannel approaches.

be followed immediately by the new sentence

> **It is worthwhile to note that those 60 points from four runs in Reference [56] are for internal rods only.**

RAI-48

48) The TR indicates in section 5.1.3.25 that the uncertainty in spray cooling heat transfer is covered by uncertainties in other parameters. However, this conclusion is not sufficiently justified. In NEDE-32177P, Revision 3, [[

]] Please reconcile the apparent conflict or provide further justification for this conclusion.

RAI-48 Response

First of all it is worthwhile to note that there is not a separate 'spray cooling heat transfer coefficient' in TRACG methodology that is applied directly. The fuel spray cooling effects, as a result of the combinations of single or two phase flow (film boiling-dispersed flow, steam cooling), radiation heat transfer and heat conduction, are calculated by modeling the physical phenomena that take place such as single phase (steam cooling) and two-phase convection , droplet evaporation, radiation to cold surfaces including droplets, Counter Current Flow Limitation (CCFL), top-down quench, etc.

[[

]]

In summary, it is concluded that there is no conflict between the uncertainty reported in NEDE-32177P, R3 for CSHT) and the PCT uncertainty reported for the BWR/2 liming break.

LTR Impact

No changes to the LTR are proposed as the result of this RAI response.

RAI-49

49) Please clarify whether the uncertainty distribution discussed in section 5.1.3.27 applies to both rising and falling quench fronts. If the uncertainty distribution applies to both, please clarify whether the uncertainty distribution database includes data from rising quench fronts. If not, please clarify how the uncertainty for rising quench fronts is addressed.

RAI-49 Response

The uncertainty described in Section 5.1.3.27 of the LTR for PIRT item C21 is applied [[ ]] The uncertainty perturbation is applied to the quench velocity as calculated from Equation (6.6-152) of LTR Reference 1 (TRACG Model Description, NEDE-32176P, Revision 4). [[ ]] The uncertainty for C21 specified in Section 5.1.3.27 of the LTR was derived on the basis of the cited falling quench data which was used to develop the NRC-approved quench model in SAFER (LTR Reference 25). [[

]]

The functional form for the quench velocity correlation is the same for both rising and falling quench fronts. In the quench velocity correlation, the leading group of dimensional quantities is based on cladding thickness and material properties that do not depend on the direction that the front is moving because they are evaluated at the cladding temperatures behind the quench front where the cladding temperature is approximately the temperature of the water. All directional dependence enters the quench velocity correlation via the Biot number defined by Equation (6.6-154) of LTR Reference 1. [[ ]] For a falling front a constant value for the heat transfer coefficient is used that was correlated from data and validated for core spray heat transfer data as described for SAFER in LTR Reference 25.

The quench model implemented in TRACG had been retained from TRAC-P1A and TRAC-BD1 and is based on the paper by Yu, Farmer and Coney identified in this response as Reference R49-1. The citation of WCAP-7435 (FLECHT) in Section 6.6.13 of LTR Reference 1 as the source of the heat transfer equation for reflood is not correct. Equation (6.6-158) of LTR Reference 1 for bottom flooding heat transfer coefficient is also incorrect. The correct expression for the bottom flooding heat transfer coefficient and a more detailed description of the TRACG quench model is available in Reference R49-2 listed below. The quench model in the TRACG code has been corrected and the corrected code will be used in all future TRACG LOCA applications. Qualification calculations related to the quench model have also been updated and the impact of the quench model on predicted PCTs have been evaluated as indicated in Reference R49-2.

Yu, Farmer and Coney (Reference R49-1) note in the introduction to their paper “that the bottom flooding correlations are consistent with the falling-film correlation for saturated flows, but that there are substantial differences where the water at the quench front is subcooled.” Later in the paper the authors note “the good agreement between bottom flooding and falling film rewetting

for saturated flows" and offer some possible explanations for why bottom flooding with subcooled water is different. It is important to stress that *agreement* is defined in Equation [9] of Reference R49-1 in terms of residual deviations between the measured wall temperature minus quench temperature compared to the correlation's prediction. In terms of the quench velocity (actually inverse quench velocity), the correlation is a best fit value of the modified Biot number in order to minimize the disagreement in temperature differences as characterized by the authors in tabulated values of σ_{min}. [[

]]

For each dataset considered in Reference R49-1, a different value of either T_0-T_s (saturated) or T_0-T_q (subcooled) was determined to minimize the variance in order to develop a best-estimate functional form of the correlation in terms of the modified Biot number. In applying the correlation a value for T_0-T_s is specified. For the 28 usable datasets from Reference R49-1 Table 5 for saturated data the values of T_0-T_s range from 17.5°C to 148.8°C with the weighted average calculated to be 74°C. [[

]] The authors of Reference R49-1 provide an average value of 67°C on page 432 of Reference R49-1 considering all saturated falling quench data from Tables 5 and 9. For all applications including saturated and subcooled fluid for falling and rising quenches the authors recommend a value of T_0-T_s=80°C since for Bi ≥ 5 "the rewetting rate is very insensitive to this parameter and the variation caused by the uncertainty in (T_0-T_q) is often much less than the experimental scatter. This is demonstrated further in Figure 18" of Reference R49-1 using "extreme values for T_0-T_s of 20°C and 160°C".

[[

]] The authors of Reference R49-1 believe that the larger uncertainty for bottom reflood (rising quench) is "entirely due to scatter in the data rather than to any inability of the theory". [[

]]

The TRACG quench model has also been evaluated for the case of a rising quench front like that observed in a reflooding situation (see Reference R49-2). Use of the TRACG quench model is

shown to result in calculated cladding temperature responses that compare well to the measured temperature responses from LOCA integral system tests where reflood quenches were experienced. [[

]]

References

R49-1 S. K. W. Yu, P. R. Farmer and M. W. Coney, *Methods and Correlations for the Prediction of Quenching Rates on Hot Surfaces*, International Journal of Multiphase Flow, 3, 1977, pp. 415-443.

R49-2 Letter J. F. Harrison (GEH) to Document Control Desk (NRC), "Update TRACG Quench Front Model Description and Qualification," MFN 13-085, October 15, 2013.

LTR Impact

No changes to the TRACG LOCA Application LTR (NEDE-33005P) are needed as the result of this RAI response. As indicated in Reference R49-2, GEH has committed to correct and enhance Section 6.6.13 of the TRACG Model Description (LTR reference [1]) and revise and augment the TRACG Qualification (LTR reference [2]) to reflect the comparisons to data obtained with the corrected quench model coding and add the new qualification cases for the Halden comparisons. All future TRACG LOCA applications will utilize the corrected code.

RAI-50

50) As shown in Figure 6-27 of NEDE-32176P, Revision 4, for post-LOCA pressures exceeding the range associated with a DEGB, the Iloeje correlation tends to predict values of the minimum stable film boiling temperature (T_{min}) that exceed other available correlations. Break spectrum calculations performed with the TRACG evaluation model suggest the possibility that small or intermediate breaks, with pressures exceeding 0.5 megapascals (MPa) during the PCT transient, could represent a potential limiting condition for some BWRs. Given that the Iloeje correlation is based only on data taken at a pressure of 6.9 MPa, it is not clear that the pressure trend in the post-LOCA range of interest can be considered reliable. It is further unlikely that the pressure-dependent trend is linked primarily to pre-existing oxidation on fuel rod surfaces. Ultimately, it is not clear that the impact of the pressure-dependent trend of the Iloeje correlation can be adequately addressed by application of [[ ]] Furthermore, the NRC staff observed that the demonstration case input decks use the Shumway correlation, which is recommended in the TRACG04P User's Manual. Based on the discussion above, please revise the model used to predict rewet and/or its uncertainty distribution, or provide adequate justification for the current approach.

RAI-50 Response

Section 5.1.3.26 of the LTR is not correct and will be updated as indicated in this response. The Iloeje correlation was not used. The Shumway correlation was used for the current LTR demonstration calculations and will be used for predicting the minimum stable film boiling temperature (T_{min}) for all future TRACG LOCA applications. Use of the Shumway T_{min} correlation with zircaloy for TRACG analyses and its qualifications are discussed and justified in Reference R50-1 (sent to NRC through GEH MFN 13-073).

Reference

R50-1 Letter, J. F. Harrison (GEH) to U. S. Nuclear Regulatory Commission, "Use of the Shumway Tmin Correlation with Zircaloy for TRACG Analyses," MFN 13-073, September 9, 2013.

LTR Impact

Reference R50-1 listed above will be added as reference [80] in Section 11 of the LTR and LTR Section 5.1.3.26 for C20 will be replaced with the text provided below. Note that this replacement text has been aligned with the response to RAI-51 where clarification and additional details are provided regarding the constraint on equilibrium quality.

5.1.3.26 C20 – Tmin (Minimum Stable Film Boiling Temperature) (H)

TRACG calculates the minimum film boiling temperature (T_{min}) using the Shumway correlation which is described mathematically by Equation (6.6-52) of Reference [1]. Comparisons of the Shumway correlation to data for a wide range of pressures are available in Section 6.6.7.3 of

Reference [1] and in Reference [80]. For the Shumway correlation, a [[
]] applied to the calculated difference between T_{min} and the saturation temperature (T_{sat}) sufficiently covers the correlation standard deviation of 55 K indicated in Reference [80]. [[

]] Although the Shumway correlation was developed using stainless steel data, it accounts for the material properties and is generally applicable for other materials (including zircaloy) as is shown in Reference [80]. A key conclusion from Reference [80] is that the Shumway correlation applied for zircaloy provides a value of T_{min} that is lower than most of the zircaloy data. Lower values of T_{min} are more conservative because they delay the return to nucleate boiling and thus result in higher and more conservative calculated values for the local cladding surface temperatures (T_{clad}).

[[

]]

The reference to be added to Section 11 of the LTR:

80 Letter, J. F. Harrison (GEH) to U. S. Nuclear Regulatory Commission, "Use of the Shumway Tmin Correlation with Zircaloy for TRACG Analyses," MFN 13-073, September 9, 2013.

RAI-51

51) As applicable to the TRACG LOCA evaluation model, please specify the circumstances under which rewetting is permitted without satisfying the requirement that the local equilibrium quality is below [[ ]] of the critical quality. In addition, please provide adequate basis for the [[ ]] The NRC staff could not locate adequate basis for these values in NEDE-32176P, Revision 4, and NEDE-32177P, Revision 3.

RAI-51 Response

In TRACG LOCA application, the local equilibrium quality below [[ ]] of the critical quality is a necessary condition for rewetting to occur. There is no circumstance under which rewetting is permitted without satisfying this local equilibrium quality requirement.

[[

]]

The uncertainties in critical quality should have no impact on non-jet pump plants (BWR/2) limiting large break scenario as the fuel bundle remains empty and the fuel rods are quenched by the falling film descending through the fuel bundles.

For jet pump plants, rewet occurs after reflood and the temperature has turned around and starts to come down. The uncertainty in the rewet has therefore no impact on the PCT. Likewise the impact on the fuel clad oxidization for jet pump plants is also minimal as the PCT is relatively low and the duration of refill/reflood phase is short.

LTR Impact

No changes to the LTR are proposed as the result of this RAI response.

RAI-52

52) In the discussion of PIRT item C22, the [[
]] Please clarify whether the intent of the discussion in section 5.1.3.28 is that heat from the channel wall may be transferred to fluid on either the inside or outside of the channel wall. It is the NRC staff's understanding that heat is transferred to fluid inside the bundle essentially only when liquid is in contact with the interior channel wall (i.e., [[ ]]). Please revise the TR, as necessary. Please provide additional explanation and justification if the NRC staff has misunderstood the quoted statement.

RAI-52 Response

In TRACG LOCA LTR calculations, heat transfer at both sides of channel wall are considered and calculated separately. Under usual LOCA conditions, heat is transferred to/from the fluid inside the channel to the channel inside wall by convection and radiation heat transfer, then across the channel wall via heat conduction, and eventually to/from the bypass fluid through the convection heat transfer on the outside of the channel wall.

The heat transfer direction either from the fluid to the wall or from the wall to the fluid depends on the local fluid temperature conditions and the channel wall surface temperature.

According to TRACG model Description in NEDE-32176P Section 6.6 (LTR Reference 1), [[

]], whenever they are applicable for particular flow regime (s) as discussed in NEDE-32176P Section 6.6.

The wording in Section 5.1.3.28 is modified as follows:

The uncertainty in channel to bypass heat transfer is covered by an [[
]] which governs **heat transfer for sub-cooled and nucleate boiling** to the inside channel wall and a [[ ]] uncertainty on wall heat transfer to the bypass which covers either nucleate boiling or single phase heat transfer.

LTR Impact

The LTR Section 5.1.3.28 will be revised as discussed above.

RAI-53

53) Please clarify the source of the data for PIRT item C24, which states that TRACG predicts the spacer component of the core pressure drop with [[
]] In contrast, Table 5-3 in NEDE-32906P, Revision 3, reports [[
]] Given the potential for increased uncertainty associated with two-phase flow throughout the bundle, please provide adequate justification for [[
]]

RAI-53 Response

The source of the data for C24 (spacer loss coefficient uncertainty) is Table 5-3 of NEDE-32906P, Revision 3 and the discussion cited therein. It is acknowledged that the sentence in the LTR [[ ]] is misleading, and therefore will be revised in the LTR.

Considering that the pressure drop measurements used for deriving the spacer loss uncertainty are already for two-phase flow, there is no increased uncertainty unaccounted for in this regard. It is acknowledged, though, that the spacer loss uncertainty is fuel design dependent. The current proposed spacer loss uncertainty shall be compared against test data for a new fuel to determine the continuous applicability of the currently-applied spacer loss uncertainty for the new fuel. The update of the current proposed spacer loss uncertainty for a new fuel may be possible.

Based on the discussion for C24 in NEDE-32906P, R3 and the biases and uncertainties for SEO/LTP, spacer, and UTP, it can also be concluded that [[
]]

LTR Impact

The following paragraph in Section 5.1.3.30 is modified in the revised LTR.

Original

A detailed discussion of the uncertainty in the frictional components of the core pressure drop was provided in the Anticipated Operational Occurrences (AOO) application report [3]. The uncertainties in the core pressure drop include the uncertainties in SEO/LTP, spacers, and UTP. Data versus TRACG-predicted pressure drop analysis indicates a
[[ ]] the core pressure drop. For the LOCA application, the uncertainty in the SEO/LTR pressure drop is considered separately (see C5 in Section 5.1.3.10) and is bounded by an uncertainty of
[[ ]] It was shown that the uncertainty in all components of the core pressure drop could be bounded by imposing a [[
]] The LOCA application uses a [[
]]

Revised

A detailed discussion of the uncertainty in the frictional components of the core pressure drop was provided in the AOO application report [3]. The uncertainties in the core pressure drop include the uncertainties in SEO/LTP, spacers, and UTP**, which are presented in Tables 5-2, 5-3 and 5-4 of Reference [3]**. ~~Data versus TRACG predicted pressure drop analysis indicates a [[ ]] the core pressure drop~~. **The spacer frictional pressure drop is based on full-scale measurement for conditions covering the range of expected reactor conditions. The uncertainty in the pressure drop for the spacers is determined from full-scale ATLAS data and is presented in Table 5-3 of Reference 3 for different fuel types. It is concluded in [3] that**
[[
]] **can be used for all bundle types.** For the LOCA application, the uncertainty in the SEO/~~LTR~~ **LTP** pressure drop is considered separately and is bounded by an uncertainty of [[ ]] (For additional discussion of the SEO/LTP pressure drop uncertainty see the response to RAI-43 and C5 in Section 5.1.3.10 of the LTR.) It was shown that the uncertainty in all components of the core pressure drop could be bounded by imposing a [[
]] The
LOCA application uses a
[[

]]

RAI-54

54) The 1979 American Nuclear Society Standard 5.1 decay heat calculation for an exposure of 15 GWd/MTU with TRACG shown in Figure 5.1-18 appears to predict decay heat power fractions that are significantly less than predictions with the same model for an exposure of 10 GWd/MTU using SAFER in NEDO-23785, Volume 3, Appendix B, Figure 1. Please clarify the different input assumptions or other causes that lead to this difference.

RAI-54 Response

The curves from Reference 54-1 for SAFER include both fission power and decay power, whereas LTR Figure 5.1-18 represents only the decay power as needed by TRACG. Recall that TRACG uses a point kinetics model to account for the fission power in the earliest stages of the LOCA whereas SAFER does not. Regrettably, the decay heat curves generated for a 0 exposure condition were mislabeled and inadvertently used for Figure 5.1-18 of the LTR. This errant figure is being replaced in the LTR by a decay heat curve generated for 11 GWd/MTU.

A new decay heat fraction was generated for 11 GWd/MTU to better match the input assumptions for the cited SAFER figure from Reference 54-1. To facilitate comparison to the SAFER figure, a plot of the fraction of the initial total power fraction (fission plus decay powers) corresponding to the new decay heat fraction is given below.

[[

]]

Reference

R54-1 NEDE-23785-1-PA, Revision 1, "The GESTR-LOCA and SAFER Models for the Evaluation of the Loss-Of-Coolant Accident", Volume 3, Appendix B, October 1984.

LTR Impact

Section 5.1.3.31 of the LTR will be revised in the following way:

(1) 15 GWd/MTU will be revised to 11 GWd/MTU.

(2) Figure 5.1-18 and its caption will be replaced with the following.

[[

]]

Figure 5.1-18 Decay Heat Uncertainty at a Bundle Average Exposure of 11 GWd/MTU

RAI-55

55) For some PIRT items, the uncertainty in future predictions of a regression model is assumed to be represented by the standard deviation associated with the data used to generate the regression model (e.g., [[
]]). Please clarify why the uncertainty associated with future predictions (i.e., data not included in the regression model) need not be determined by the prediction interval for a new observation. See, for example, section 18.17 of NUREG-1475, Revision 1.

RAI-55 Response

As stated in Section 18.17 of NUREG-1475 (Revision 1) a regression equation provides only a prediction Y' for an expected value Y. It is understood that multiple samples from the same regression equation using the same inputs will always return the same prediction Y'. In a broader context a "regression model" is expected to behave in the same way. In the broadest context, a digital computer code also operates in this way by providing a set of predicted values that are determined once the set of inputs are specified. The term "regression model" used in RAI suggests a purely empirical fit of numbers that has been tuned to a small dataset and that the addition of data will require retuning. This characterization minimizes the importance of physical bases for the model functional form, the choice of dimensionless engineering parameters that represent fundamental processes, and even the type and range of allowed inputs. The key generic principle is that there exists a defined process that adequately transforms inputs into outputs whether that process is a simple regression equation, a regression model, or a computer code. Adequacy of the process and the outputs it produces are quantified together by defining tolerance limits for the critical outputs that reflect both the fidelity of the transformation process and the uncertainty of the inputs. Whenever possible, it is the calculated output that is compared to data and it is this comparison that determines whether the process and/or its inputs are in need of improvement. Rarely is it necessary to increase the uncertainty of the inputs to provide for a wider spread in the calculated outputs to adequately cover the data.

The RAI suggests using the prediction interval for the regression equation instead of the standard deviation to characterize the uncertainty of the prediction. This is not the correct application of the prediction interval. What is needed for application of Best Estimate Plus Uncertainty (BEPU) methodology is a way to model the variance of the sampled predicted values about the expected value. The appropriate statistical parameter that defines this variance is the standard deviation (σ), not the prediction interval. The prediction interval is defined from the standard deviation not vice versa. As the number of data points increases the standard deviation may tend to decrease slightly but more importantly the confidence increases which decreases the prediction interval. Thus modeling the variance of a population to be sampled based on a small number of data points tends to provide a conservatively larger variance in the model inputs. If new data becomes available then this data is evaluated to determine its impact on the biases and uncertainties used in the LOCA application methodology.

For BEPU the objective is to evaluate the uncertainty associated with complex interactions between many competing processes with many different inputs. In the BEPU methodology the ultimate concern is whether the final estimated uncertainty in the calculated critical output parameter is sufficient to cover the experimental data for the critical parameter. These types of coverage checks for the final outputs are more important than the span of particular inputs.

It is not clear from the RAI whether the concern is with *coverage* for the inputs or the outputs so both aspects are addressed. Begin with the more important aspect of uncertainty in the output critical parameters. The process is described in Section 7.1 of the LTR. A one-sided upper tolerance limit (OSUTL) is defined for each of the three critical parameters: (1) PCT, (2) maximum local oxidation, and (3) total core-wide oxidation. These three OSUTLs are defined independently for each set of 59 calculations using either a single bounding value based on order statistics (LTR Section 7.1.1) or a calculated OSUTL from a normal distribution (LTR Section 7.1.2). In either case the OSUTL is defined to provide at least 95% probability at 95% confidence that the OSUTL bounds the calculated population. The maximum OSUTL from all sets of calculations is compared to the appropriate 10 CFR 50.46 design limit independently for each of the three critical parameters as described in Section 7.4 of the LTR. This is done without any requirement or assumption regarding simultaneity of the maximums thus assuring that each maximum is less than 10 CFR 50.46 limit with a high degree of probability. The population of calculated outputs does not change unless new scenarios are required or new inputs are specified.

The statistical process used for BWR LOCA calculations has been applied to relevant integral system tests where generally the PCT and some other parameters of interest have been measured. Comparison of the calculated tolerance limits to the measured data demonstrates the adequacy of the BEPU approach. See Section 7.4 of the LTR for the specific results.

Next consider coverage for the inputs. For the cited examples of C21 and C26, models based on physical processes provide the expected values for the derived input quantities. These derived inputs are uncertain because the models used to obtain them are uncertain and even the inputs to these models that create other inputs are also uncertain. In accordance with the BEPU methodology, the sample for an input represents a best-estimate value distributed in some way about the mean (μ). The confidence interval for the mean is always much tighter than the individual samples. The concern with input *coverage* is addressed by considering over what range the sampled inputs are drawn. For GEH BEPU applications we typically use [[ ]] to assure adequate ranging of the uncertain inputs unless there is a physical constraint that limits the range to something smaller. The span for the inputs in GEH methodology is greater than the range needed to assure coverage of the inputs beyond the 95% confidence interval unless the input uncertainty was determined from a very small number of data points (less than 6). The next paragraph provides a specific example to illustrate why this process is adequate for purposes of providing input coverage.

Consider the particular example of C21 cited in the RAI. In Figure 5.1-17 of the LTR, the reported mean is [[ ]] with a 95% confidence interval on the mean of [[ ]] The standard deviation is [[ ]] and the 95% confidence interval for the standard deviation is reported as [[ ]] data points. In GEH BEPU

modeling the sampling interval spans [[ ]] which for this example is [[ ]]. By way of comparison, consider the prediction interval defined by Equation (18.60) of NUREG-1475 (Revision 1). If the regression equation is assumed to be linear to simplify the calculations then the mean value of the independent variable will produce the mean value of the dependent variable. At the mean of the independent variable where x=xbar, the 95% confidence interval about the predicted mean value for the dependent value of y reaches a minimum span. The confidence interval expands slightly as the independent variable moves away from the mean but this expansion (which is greater when the database has fewer values) is negligible as illustrated in Figure 18.10 for n=11. For the C21 example where the database has [[ ]] a two-sided 95% confidence interval for a Student's t-distribution with (n-2) degrees of freedom produces a 95% confidence interval span $\pm 2\sigma$ about the mean that covers [[ ]] GEH sampling has adequate coverage because it spans [[ ]] about the mean and covers [[ ]]

The BEPU statistical approach proposed and demonstrated in the LTR is justified because it provides a high probability that the 10 CFR 50.46 limits are not exceeded by: (1) adequately addressing the input biases and uncertainties, (2) accounting for the modeling biases and uncertainties, and (3) accounting for the uncertainty in the calculated outputs due to both input and modeling biases and uncertainties.

LTR Impact

No changes to the LTR are proposed as the result of this RAI response.

RAI-56

56) Based on the data plotted in Figure 5.1-19, it is not clear that a normal distribution explains the variation in predictions of the single-parameter model used for pre-accident oxidation. Please provide the Anderson-Darling normality test results for C26I (initial oxide thickness) and justify that the assumption of normality does not result in significant error relative to the criteria of 10 CFR 50.46.

RAI-56 Response

The variation in predictions of the exposure-dependent pre-transient oxidation (PTO) model are explained by the nominal and 95%-content tolerance limit curves presented in Figure 5.1-19 of the LTR. Using these curves, a statistical sampling model is generated where half-normal distributions between the nominal and $\pm 2\sigma$ tolerance limits are joined at each exposure. To show the comparison of the resulting model to metallographic data, each oxidation thickness t_i at exposure E_i is transformed to a z-value z_i using the exposure-dependent model values $t(E_i)$, $t_{LTL}(E_i)$, and $t_{UTL}(E_i)$ with the following relationship.

$$z_i = \begin{cases} 2\left(\dfrac{t_i - t(E_i)}{t(E_i) - t_{LTL}(E_i)}\right), & t_i < t(E_i) \\ 2\left(\dfrac{t_i - t(E_i)}{t_{UTL}(E_i) - t(E_i)}\right), & t_i \geq t(E_i) \end{cases}$$

A histogram of the z-values is presented in Figure R56-1. The transformed metallographic data are compared here to a standard normal distribution, although the data's Anderson-Darling p-value of 0.010 does not justify normality. It is shown, however, that the preponderance of the data is bounded by the standard normal distribution. This can be observed both in Figure R56-1 and in the cumulative distribution functions in Figure R56-2. In both figures, positive z-values indicate that the model PTO is greater than the observed data. A statistical calculation using this model therefore predicts a bounding distribution of pre-transient oxidation thickness values.

Furthermore, the oxidation thickness levels presented in Figure 5.1-19 of the LTR are on the order of 0.2-2% of GE14 fuel cladding thickness for the exposures of interest in LOCA analysis. The BWR/2 DBA demonstration results presented in Figure 8.3-29 of the LTR show an upper tolerance limit oxidation thickness on the order of 8%, with 9% margin to the 10 CFR 50.46 criteria. It is therefore justified that the assumptions surrounding PTO do not result in significant error relative to the margin to the oxidation limit.

LTR Impact

No changes to the LTR are proposed as the result of this RAI response.

[[

]]

Figure R56-1 Histogram of Pre-Transient Oxide Thickness Z-Values

[[

]]

Figure R56-2 Cumulative Distribution of Pre-Transient Oxide Thickness Z-Values

RAI-57

57) The basis for the adequacy of the database used to derive the uncertainty distribution for critical flow is not clear, and the uncertainty proposed by GEH appears substantially lower than other statistical studies. Please either revise the uncertainty distribution proposed in section 5.1.11.1 in response to the concerns below, or provide adequate justification that the proposed distribution remains appropriate in light of these concerns:

a. A large body of critical flow data exists; however, only nine tests were used to derive the uncertainty parameters for the TRACG LOCA evaluation model. The limited dataset is particularly important because critical flow behavior and uncertainties vary significantly across various flow regimes (e.g., subcooled, saturated liquid, two-phase, steam). Because the chosen tests appear to have been selected to span these flow regimes, the proposed uncertainty distribution resembles an amalgamation of even smaller samples from several distinct populations, rather than a statistical treatment of a single population. (The dependence of uncertainty on the flow regime is alluded to in section 6.3.6 of NEDE-32176P, Revision 4, which references a slightly larger database of eleven tests.) As such, the amalgamated uncertainty distribution proposed by GEH includes single-phase data, which downwardly biases the uncertainty in the critical flow rate for the limiting recirculation breaks where larger two-phase uncertainties dominate.

b. The basis for the selection of the nine tests used to derive the proposed uncertainty distribution (or, equivalently, the rejection of other applicable tests) from the large body of existent critical flow data has not been justified. In particular, some of the test data chosen to derive the uncertainty distribution (e.g., the comparison with GIRAFFE break flow at twenty minutes) does not appear to be among the most applicable with regard to simulating the limiting LOCA scenarios expected for operating BWRs.

c. The basis for choosing specific datapoints from a given test for comparison, as well as the weighting of data during the statistical combination process is not clear. Uncertainty associated with times early in the blowdown (e.g., for a large break) can be higher and further is apparently more influential on PCT than uncertainty at later times.

d. As applicable, please discuss the selection of critical flow discharge coefficients for the statistical database used to derive the uncertainty distribution and to what extent latitude in making this choice influences the statistical results. Please further clarify how discharge coefficients will be chosen for plant-specific analysis.

e. Please clarify the significance of noncondensibles on critical flow and the consequent impact on figures of merit for the LOCA evaluation model. If significant, please further discuss the validation of the models used for noncondensibles and identify whether the influence of noncondensibles is included in any of the tests in the statistical database.

RAI-57 Response

GEH disagrees with the premise that the uncertainty for critical flow proposed by GEH is substantially lower than the uncertainties from other statistical studies, particularly when compared to other realistic LOCA methodologies approved in the U.S. See the discussion below in part (a).

a) The TRACG critical flow model has been qualified, based on the test data discussed in the LTR. Those data points cover the whole spectrum of critical flow, spanning from liquid break to steam flow. The current TRACG critical flow uncertainty is then derived from those data. The maximum is used.

Although the assessment of the TRACG critical flow model uncertainty was limited to those representative test data considered to be the most appropriate, the model was developed using amalgamated data that spans the entire range of pressure and flow conditions. There is not a substantial difference in the uncertainty distribution of the critical flow discharge coefficient (CD) used in other approved realistic LOCA methodologies compared to the critical flow uncertainties used in the TRACG model. As discussed in LTR Section 5.1.11.1, the current GEH LOCA methodology [[

]] For comparison, based on the information obtained from References R57-1 and R57-2, the CD in one methodology ranges from 0.80 to 1.40, a spread of 0.60 between the min and max. Therefore, no substantial difference appears to exist in the applied uncertainties for the GEH methodology.

Similarly, another approved methodology appears to sample from -2-sigma to +2-sigma (or from the min to the max) for critical flow modeling, based on the information gathered from Reference R57-3. Further, the break critical flow uncertainty in this model seems to also be based on multiple data points from the 9 Marviken tests (See Table 3 and Figure 3 in Reference R57-3).

Significantly, the selection of various break sizes addresses any concern regarding the critical flow uncertainty when there is sufficient overlap between neighboring analysis points. The current TRACG LOCA methodology follows a procedure that would find the break type and location, which would result in the highest PCT.

When break flow is choked at the break location, the break flow uncertainty can be sufficiently compensated by varying the break sizes. Since the system response is primarily related to the total inventory loss through the break with other inputs unchanged, the same inventory loss through the break would result in similar system response (pressure, temperature and the PCT). Therefore, a break area increase while simultaneously reducing the break flow rate, or the break area decrease while simultaneously increasing the break flow rate, so that the total break flow rates are essentially the same would generate essentially the same LOCA response, and thus essentially the same PCT. The critical flow increase (or decrease) due to critical flow uncertainties is, therefore, equivalent to a break size increase

(or decrease) by an amount so that their product remains the same. The inconsequential effect of the critical flow uncertainties on limiting break size and PCT in break spectrum calculations can be demonstrated.

In the following sections, sensitivity studies are made regarding the above discussion and conclusion. In these sensitivity runs, the break critical flow is [[

]]

BWR/4

Using the detailed core channel model discussed in RAI-6, the BWR/4 recirculation suction line breaks are analyzed at 0.02, 0.07, 0.4, 0.67, 2.0 ft^2, and the maximum area split and DEGB (7.1 ft^2). For each break, 11 TRACG runs are performed with different critical flow multipliers. The core PCTs for each break are presented in Figure R57-1. For each break size (A_{break}), the PCTs from all 11 runs with different critical flows are paired with the so-called equivalent break area, which is $CD*A_{break}$. The pairs of PCTs and the equivalent break areas are plotted in Figure R57-1. Included in this figure is the break spectrum, which is obtained with the nominal critical flow.

It can be observed from the results presented in Figure R57-1:

[[

]]

[[

]]

Figure R57-1 BWR/4 Break Spectrum for Recirculation Line Suction Breaks with Battery Failure

BWR/2

Using the detailed core model discussed in RAI-9, the BWR/2 recirculation discharge line breaks are analyzed at 0.05, 0.3, 3.0 ft^2, and the maximum area split break and DEGB (7.2 ft^2). The calculation and the process procedure for BWR/2 is the same as that for BWR/4 in the previous section. The pairs of the core PCTs and the equivalent break areas for BWR/2 discharge break are plotted in Figure R57-2. Included in this figure is the break spectrum, which is obtained with zero critical flow uncertainties.

It can be observed from the results presented in Figure R57-2:

[[

]]

[[

]]

Figure R57-2 BWR/2 Break Spectrum for Recirculation Line Discharge Breaks

In summary, the current critical flow uncertainties used for the TRACG LOCA methodology are comparable to the range adopted for other major US reactor vendors. Furthermore, the sensitivity studies have demonstrated that the selection of various break sizes addresses any concern regarding the critical flow uncertainty with sufficient overlap between neighboring analysis points. Extending the current critical uncertainties to a larger range has insignificant impact on the current method.

The current critical flow uncertainty distribution is therefore justified for the applications.

b) The TRACG LOCA methodology is not sensitive to the critical flow uncertainty. See the discussion in Item a.

c) The TRACG LOCA methodology is not sensitive to the critical flow uncertainty. See the discussion in Item a.

d) Unlike other applications using discharge coefficients (CD), there is no tuning of CD to match results in the GEH TRACG LOCA methodology. Applications will calculate the

critical flow for the break area of interest and sample directly from the uncertainty distribution for the critical flow as given in the LTR.

e) It has been found from the demonstration calculations in the LTR that the noncondensable gas does not infiltrate into the system for BWR/4 and BWR/6, and therefore, the current LOCA model is not impacted by the noncondensable gas from the outside. For BWR/2, ambient noncondensable gas has been found to have significant impact on the core channel LOCA responses (PCT and oxidation). However, by the time the ambient noncondensables are a significant portion of the vessel inventory by means of ingress through the break, the discharge is no longer choked. Therefore, the ambient noncondensables impact on critical flow is inconsequential. (This is unlike PWR LOCA scenarios where the accumulators discharge nitrogen into the RCS while the pressure is still high enough that the flow of nitrogen through the break can influence the critical flow.)

   During normal operation, there would be some small amount of noncondensable gases in the system due to radiolysis. Those noncondensables will be primarily in the gas space. Their impact on the liquid breaks, which are the limiting breaks for all plant types, is inconsequential.

   Another source of noncondensables inside the system is due to the metal water reaction. This reaction happens at high cladding temperatures and occurs usually at the later phase of the LOCA (Significant metal-water reaction is not expected for BWR/4 and BWR/6 LOCAs). Therefore, by the time the inside noncondensables are significant to the LOCA response, the discharge flow through the break is no longer choked. Therefore, the noncondensables generated during the LOCA do not impact the current critical flow and figures of merit for the LOCA evaluation model.

References

R57-1. K. Takeuchi and M. E. Nissley, "Best Estimate Loss-of-Coolant Accident Licensing Methodology Based on WCOBRA/TRAC Code," International Meeting on 'Best-Estimate' Methods in Nuclear Installation Safety Analysis, BE-2000, Washington DC, November 2000.

R57-2. K. Takeuchi and M. E. Nissley, "Uncertainty Evaluation of Global Model Combined with Local Hot Spot Response Surface in the WCOBRA/TRAC BE Method," International Meeting on 'Best-Estimate' Methods in Nuclear Installation Safety Analysis, BE-2000, Washington DC, November 2000.

R57-3. R.P. Martin and L.D. O'Dell, "Development Considerations of AREVA NP Inc.'s Realistic LBLOCA Analysis Methodology," Science and Technology of Nuclear Installations, Volume 2008.

LTR Impact

No changes to the LTR are proposed as the result of this RAI response.

RAI-58

58) The basis for the attribution in section 5.1.6.2 of all uncertainty associated with PIRT item F2 to the uncertainties associated with liquid side interfacial heat transfer and drag is unclear. For example, as discussed in section 7.8.2 and section 7.8.3 of NEDE-32176P, Revision 4, the modeling of injected spray and turbulent mixing both influence upper plenum mixing. Please justify the insignificance of these parameters or include them as factors in the uncertainty analysis for PIRT item F2.

RAI-58 Response

The premise of the question is that item F2 is important. This is not the case. The dominant impact of ECC interaction in the upper plenum is to change the upper plenum pressure and the temperature of the spray water. The ECC spray has a very large heat transfer surface area which over a short distance causes the sprayed water to increase in temperature to the saturation temperature. The speed at which this is done is dominated by the liquid side interfacial heat transfer. Interfacial drag is also important because it determines the ability of steam passing thru the upper plenum to carry spray drops upward and away from the core. These are the phenomena treated by F2.

Other important phenomena important to determining the LOCA licensing parameters are addressed in other ways. Ultimately, the key quantity that must be determined is how much of the water available in the upper plenum makes it down into the core. For this purpose the modeling of the spray distribution in the upper plenum (F4) is relevant for as long as the spray header is uncovered. A conservative approach based on experimental data was used in the LTR demonstration calculations. Spray distribution (F4) is the most important for BWR/2 calculations where the dominant flow path through the core is downward.

For jet pump plants, Counter Current Flow Limitation (CCFL) at locations near the top of the core (B5, C7) tends to hold up water in the upper plenum resulting in a pool that rises to cover the spray sparger. Once the spray sparger is approaching submergence the steam heating of the spray is diminished to the point that the upper plenum pool (if present) begins to subcool and CCFL breakdown (B5,C7) occurs allowing draining of water into the core first into the bypass then directly into the fuel bundles. The flow of water from the bypass into the fuel bundles is also important (B6, B9, C11).

The application of all these models is integrated with nodalization sensitivity studies and test results from integral facilities to provide a somewhat conservative evaluation of the fluid inventory in the fuel channels. What is actually conservative in terms of fluid inventory is complicated. It is one of the main reasons that it is necessary to perform a break spectrum analysis and quantify the uncertainty in PCT as a function of the break size.

LTR Impact

No changes to the LTR are proposed as the result of this RAI response.

RAI-59

59) Please provide Anderson-Darling normality test descriptive statistics for PIRT item F3. Please further clarify whether the correlation for turbulent films is of importance for the uncertainty analysis for a LOCA and whether this regime was covered by tests used to derive the uncertainty distribution or is otherwise accounted for by the TRACG evaluation model.

RAI-59 Response

The uncertainty associated with PIRT item F3, Noncondensable Return at Low Pressure, is assessed by estimating the uncertainty of the noncondensable degradation factor applied to the liquid-side interfacial heat transfer coefficient. The degradation factor is given in Eq. 6.5-28 of the TRACG Model Description report (LTR Reference [1]) and is reproduced here for convenience.

$$C_{ncg} = \min\left\{1.0, 0.168\left(\frac{\alpha\rho_s^2}{(1-\alpha)\rho_a\rho_l}\right)^{0.1}\right\} \quad \text{(R59-1)}$$

As noted in Section 5.1.6.3 of the LTR, the uncertainty of this degradation factor is estimated by examining the known uncertainty from a separate relationship involving condensation degradation, the Kuhn-Schrock-Peterson (K-S-P) correlation. The uncertainty of the noncondensable degradation factor is approximated by the uncertainty in the heat transfer coefficients from the K-S-P, because the degradation mechanism across the applications is essentially the same.

It is therefore not possible to provide descriptive statistics for PIRT item F3, as the uncertainty is estimated from another application, not from application-specific test data. For further information, the data that is used to derive the uncertainty of the K-S-P correlation is presented graphically in Figure 3.6-3 of Reference R59-1.

As demonstrated in Figures 8.3-11, 8.3-12, and 8.3-13 of the LTR, liquid-side heat transfer degradation due to noncondensables has a Spearman correlation factor with PCT of less than 0.4, and is therefore not a significant factor in PCT performance in BWR/2 accident scenarios.

Reference

R59-1 W.R. Usry, “Single Tube Condensation Test Program,” NEDC-32301, GE Proprietary Report, March 1994.

LTR Impact

No changes to the LTR are proposed as the result of this RAI response.

RAI-60

60) Please clarify the pressure drop parameter that is varied for PIRT item H4 (pump pressure drop) in the LOCA evaluation model and specify the uncertainty distribution and parameters along with justification. Please further identify the number of tests that were considered in the derivation of the uncertainty assumptions, and summarize the test conditions and the basis for their applicability to LOCA conditions.

RAI-60 Response

The uncertainty in the recirculation pump pressure drop (PIRT item H4) was dispositioned by treating the modeled homologous pump curves as a plant parameter. In particular, the sensitivity of the limiting BWR/4 break scenario to the modeled pump curves has been evaluated. [[

]]

LTR Impact

No changes to the LTR are proposed as the result of this RAI response.

Table R60-1 Pump Curves Sensitivity Results for BWR/4 Limiting Break Scenario
[[ ]]

Case	[[	]]
Mean (K)		
Standard Deviation (K)		
Normal?		
Maximum (K)		

[[

]]

Figure R60-1 Limiting BWR/4 Break PCT with [[ ]]

[[

]]

Figure R60-2 Limiting BWR/4 Break PCT with [[ ]]

RAI-61

61) For PIRT item M8, an effective reduction is proposed for its uncertainty relative to NEDE-32906P. However, under LOCA conditions, a greater uncertainty may actually be expected because (1) the peak mass flow rates during blowdown may exceed flows during normal operation (especially for the BWR/2 design) and (2) the flow is two-phase. Please clarify the extent to which these two factors are accounted for in the database used to derive the proposed uncertainty distribution, and if necessary revise the uncertainty distribution.

RAI-61 Response

Ranking of the phenomenon as high or medium is with respect to the expected impact on the critical safety parameters that are different for Anticipated Operational Occurrences (AOO) and LOCA applications. The distinction between a high and medium ranking is not relevant because for either high or medium rank the applied uncertainty is the same. The uncertainty in the correlations is determined from data that also cover the LOCA application range. Section 6.2 of TRACG Model LTR (NEDE-32176P, R4) shows that both wall friction and local form losses account for two-phase effects. The wall friction is also a function of Reynolds number. The [[ ]] is on the coefficient so that the absolute pressure drop uncertainty proportionally increases for higher flows expected for LOCA blowdown conditions. The amount of the applied uncertainty was confirmed by application to multiple integral tests including FIST and SSTF as discussed in Section 7 of the LTR. Therefore, there is no need to revise the uncertainty distribution.

LTR Impact

No changes to the LTR are proposed as the result of this RAI response.

RAI-62

62) The TR proposes in section 5.1.13.2 a range for isolation condenser heat transfer [[ ]] If isolation condensers are credited for the limiting LOCA scenario for a given plant, please commit to validating that this distribution is appropriate on a plant-specific basis for future licensing calculations and revise the TR to state as such.

RAI-62 Response

As stated in Section 8.3.2.1 of the LTR, a single failure resulting in the loss of an isolation condenser is postulated (see the response to RAI-32 also). Furthermore, the remaining isolation condenser is not credited. Sections 5.1.13.2 and 8.3.2.1 and Table 5.1-2 of the LTR will be revised to reflect this statement. If the isolation condenser is to be credited, we commit to validate the distributions that are appropriate on a plant-specific basis.

LTR Impact

Sections 5.1.13.2 and 8.3.2.1 and Table 5.1-2 of the LTR will be revised as discussed in this response.

RAI-63

63) In May 2004, BWR/2 licensees submitted 10 CFR 50.46 notifications that refer to an exothermic hydrogen-oxygen recombination reaction having the potential to increase the calculated PCT and local oxidation. The phenomenon appears to have been dispositioned, in part, based on the conservatism inherent in the Appendix K evaluation model. Please discuss and provide justification if the hydrogen-oxygen recombination phenomenon is deemed insignificant for BWR/2s in the context of the best-estimate TRACG evaluation model.

RAI-63 Response

The issue that was first reported in May 2004 regarding the hydrogen recombination was based on an unrealistic conservative assumption that the hydrogen produced by the zirconium-steam reaction remains in close proximity with the cladding and reacts with oxygen from an unknown source of unlimited air without being displaced by that air or steam. Overly conservative and unrealistic assumptions of this type may be construed by some as being consistent with the philosophy of Appendix K evaluation models. Such an assumption is not appropriate for realistic best-estimate modeling. The scenario is not realistic because all U.S. BWR/2s have containment designs that are inerted with nitrogen and the amount of available oxygen is insufficient. Therefore, there is no credible mechanism to recreate a scenario as described for BWR/2s which have inerted Mark-I containments.

LTR Impact

No changes to the LTR are proposed as the result of this RAI response.

RAI-64

64) Please clarify the method used to derive the uncertainty bands for the CCFL constant, K, for PIRT items C6 and C7 and provide the following references:

a. D.D. Jones, "Subcooled CCFL Characteristics of the Upper Region of a BWR Fuel Bundle," NEDG-23549, July 1977.

b. D.D. Jones, S.S. Dua, "GE Analytical Model for LOCA Analysis in Accordance with 10CFR50 App. K; Amendment 4 – Saturated CCFL Characteristics of a BWR Upper Tieplate," NEDE-20566-4-P, July 1978.

RAI-64 Response

For the side entry orifice (SEO) Counter Current Flow Limitation (CCFL), item C6, the uncertainty is defined by the distribution of the difference between the value of CCFL constant used in the TRACG model, $K_T^{1/2}$, and the measured values from tests, $K_E^{1/2}$. In particular, the side entry orifice (SEO) CCFL test data is shown on Figure 13 of Reference R64-1. The default TRACG $K^{1/2}$ value for this location is [[ ]] For each test point, an experimental $K^{1/2}$ value is determined by adding the abscissa and ordinate values. The uncertainty reported in the LTR is then defined by the resulting distribution of ($K_T^{1/2}$ - $K_E^{1/2}$)/ $K_T^{1/2}$ from these test points.

For the upper tieplate (UTP) CCFL uncertainty, item C7, the input constant is a function of fuel product line. The detailed discussion for UTP CCFL was presented in References R64-1 and R64-2. For the UTP uncertainty, [[

]]

Electronic versions of the documents referenced herein as well as the copies of the requested documents are provided.

References

R64-1 NEDE-13430, "Calculation of Counter-Current Flow Limiting Conditions in BWR Geometry," September 1975.

R64-2 NEDE-20566-4-P, "GE Analytical Model for LOCA Analysis in Accordance with 10CFR50, App. K; Amendment 4 – Saturated CCFL Characteristics of a BWR Upper Tieplate," July 1978.

LTR Impact

No changes to the LTR are proposed as the result of this RAI response.

RAI-65

65) Section 7.1.1 of the TR states that continuity in the probability density functions for figures of merit is a requirement for determining non-parametric tolerance limits according to Wilks' Theorem. However, it is not obvious that these probability density functions will, in general, be continuous. In fact, [[ ]] calls the TR's assumption of continuity into question. Therefore, please demonstrate that the requirement for continuous probability density functions will be satisfied in the application of the evaluation model described in the TR for quantifying a single probabilistic statement of safety for the complete spectrum of break locations and sizes, the complete spectrum of model parameters and their variation, and the nonlinear feedback introduced by the engineered safety features. In other words, please show that there are no disjoint density functions of the figures of merit, or they can be identified and taken into account in the application of Wilks' Theorem.

RAI-65 Response

Continuity of the probability density functions for figures of merit is not a requirement for determining the non-parametric tolerance limits. Although the original work by Wilks is based on continuity of the probability density function, Wald's work further extends the method to discrete distributions (Reference R65-1). As demonstrated in RAI-6 and RAI-9 responses, the bifurcated behavior is effectively eliminated from the computed results. The simulations performed to date support that the probability density functions for figures of merit are practically from continuous functions. The methodology does not depend on a continuity requirement. Therefore the sentence regarding this aspect being a requirement will be removed.

Reference

R65-1 A. Wald, "An Extension of Wilks' Method for Setting Tolerance Limits," *The Annals of Mathematical Statistics*, Volume 14, Issue 1, March 1943, 45-55.

LTR Impact:

Following sentence from Section 7.1.1 of the LTR will be removed:

"The only requirement for the validity of the OSUTL derived in this manner is continuity of the PDFs providing the samples for each trial."

RAI-66

66)

(a) Please justify the conclusion made in the TR that 59 code simulations is sufficient to establish joint 95/95 upper tolerance limits for all pertinent criteria of 10 CFR 50.46 (i.e., PCT, local oxidation, and core-wide oxidation) using non-parametric order statistics. For background, please refer to the discussion provided in the NRC staff's review of a similar statistical approach (ADAMS Accession No. ML062150349).

(b) Please justify the conclusion that assessing compliance with the criteria of 10 CFR 50.46 on an individual basis using a combination of parametric and non-parametric statistical approaches is capable of assuring that 95/95 limits are jointly satisfied. Please further justify that choosing between the parametric and non-parametric approaches *a posteriori* does not degrade the intended confidence level.

RAI-66 Response

The TRACG LOCA methodology conforms to 10 CFR 50.46(a)(1) which states:

> "… Except as provided in paragraph (a)(1)(ii) of this section, the evaluation model must include sufficient supporting justification to show that the analytical technique realistically describes the behavior of the reactor system during a loss-of-coolant accident. Comparisons to applicable experimental data must be made and uncertainties in the analysis method and inputs must be identified and assessed so that the uncertainty in the calculated results can be estimated. This uncertainty must be accounted for, so that, when the calculated ECCS cooling performance is compared to the criteria set forth in paragraph (b) of this section, there is a high level of probability that the criteria would not be exceeded. …"

Regulatory Guide 1.157 also states that a 95% probability level is considered acceptable for comparison of best-estimate predictions to the applicable limits. There is no defined requirement for the confidence interval associated with the upper one-sided probability limit. RG 1.157 states (highlighting added for emphasis):

> "4.4 Statistical Treatment of Overall Calculational Uncertainty
>
> The methodology used to obtain an estimate of the overall calculational uncertainty at the 95% probability limit should be provided and justified. If linear independence is assumed, suitable justification should be provided. The influence of the individual parameters on code uncertainty should be examined by making comparisons to relevant experimental data. Justification should be provided for the assumed distribution of the parameter and the range considered.
>
> In reality, the true statistical distribution for the key parameters (e.g., peak cladding temperature) is unknown. The choice of a statistical distribution should be verified using applicable engineering data and information. **The statistical parameters appropriate for that distribution should be estimated using**

available data and results of engineering analyses. Supporting documentation should be provided for this selection process. These estimated values are assumed to be the true values of the statistical parameters of the distribution. With these assumptions, an upper one-sided probability limit can be calculated at the 95% level. As the probability limit approaches 2200°F, more care must be taken in the selection and justification of the statistical distribution and in the estimation of its statistical parameters. **If a normal distribution is selected and justified, the probability limit can be conservatively calculated using two standard deviations.** The added conservatism of the two standard deviations compared to the 95th percentile is used to account for uncertainty in the probability distribution. Other techniques that account for the uncertainty in a more detailed manner may be used. **These techniques may require the use of confidence levels, which are not required by the above approach.**

The evaluation of the peak cladding temperature at the 95% probability level need only be performed for the worst-case break identified by the break spectrum analysis in order to demonstrate conformance with paragraph 50.46(b). However, in order to use this approach, justification must be provided that demonstrates that the overall calculational uncertainty for the worst case bounds the uncertainty for other breaks within the spectrum. It may be necessary to perform separate uncertainty evaluations for large- and small-break loss-of-coolant accidents because of the substantial difference in system thermal-hydraulic behavior.

The revised paragraph 50.46(a)(1)(i) requires that it be shown with a high probability that none of the criteria of paragraph 50.46(b) will be exceeded, and is not limited to the peak cladding temperature criterion. **However, since the other criteria are strongly dependent on peak cladding temperature, explicit consideration of the probability of exceeding the other criteria may not be required if it can be demonstrated that meeting the temperature criterion at the 95% probability level ensures with an equal or greater probability that the other criteria will not be exceeded.**"

a. In the regulation, 10 CFR 50.46 and RG 1.157, there is no requirement for a "joint" 95/95 upper tolerance limits. Therefore, the expectation that peak cladding temperature, maximum local oxidation, and core-wide oxidation limits to be met jointly is in excess of current licensing requirements. Furthermore, GEH methodology already meets or exceeds the number of runs required for 95/95 upper tolerance limits as described in ML062150349. The similar statistical approach discussed in that reference utilizes break sizes sampling. When compared to the methodology and its statistical approach discussed in ML062150349 on an equal basis, GEH is running minimum of 177 (3 times 59) cases to obtain an equivalent PCT for the break sizes in consideration. This already exceeds the number of runs expected.

The process used by GEH is described in Section 7.1 of the LTR. A one-sided upper tolerance limit (OSUTL) is defined for each of the three critical 10 CFR 50.46 parameters: (1) PCT, (2) maximum local oxidation, and (3) total core-wide oxidation. These three OSUTLs are defined independently for each set of 59 calculations using either a single bounding value based on order statistics (LTR Section 7.1.1) or a calculated OSUTL from a normal distribution (LTR Section 7.1.2). In either case the OSUTL is defined to provide at least 95% probability at 95% confidence that the OSUTL bounds the calculated population for each critical parameter based on the specific scenario (break size/location and equipment). The maximum OSUTL from all sets of calculational scenarios is determined for each critical parameter and is compared to the appropriate 10 CFR 50.46 design limit independently for each of the three critical parameters as described in Section 7.4 of the LTR. This is done without any requirement or assumption regarding simultaneity of the maximums thus assuring that each maximum is always less than its specific 10 CFR 50.46 limit with a high degree of probability.

GEH further studied the impact of running 124 cases instead of 59 on the calculated one-sided upper tolerance limit (OSUTL). The BWR/4 simulations performed using the detailed core model described in the RAI-6 response are used as an example. A new random set of inputs were prepared and 124 simulations were carried out. Table R66-1 summarizes the figures of merit (FOMs) from that study. Consistent with the methodology, the OSUTL values in the table are either calculated using the mean and the standard deviation if the distribution is not non-normal, or set to be equal to the maximum value as in order statistics.

The study further demonstrates that 59-case statistical analysis is sufficient in determining 95^{th} percentile PCT, Maximum Local Oxidation (MLO), and Core Wide Oxidation (CWO) with high probability and 124-case statistical analysis is not necessary to achieve similar outcome. Furthermore, by analyzing small, intermediate, and large breaks separately using a total of 177 runs, GEH methodology exceeds the expectation NRC imposed on other approved realistic LOCA methodologies.

Table R66-1 Statistical Summary Comparison Between 59 and 124 Cases: BWR/4 0.67 ft^2 Break

		59 cases	124 cases
Peak Cladding Temperature (K)	[[		
Maximum Local Oxidation (ECR)			
Core-wide Oxidation			
			]]

Notes: For normal distributions, OSUTL values are calculated using mean+(z-value)(std.dev); z-value for 59 cases is 2.024, and for 124 cases, it is 1.892. PCT values are rounded up to a whole number. For non-normal distributions, OSUTL is determined from the highest value for 59 cases, and the 3rd highest for the 124 cases.

b. The statistical tests using limited quantity of random samples from an unknown distribution provide statistical information regarding true distribution with a certain level of confidence. When the random sampling takes place, there is no predetermined distribution function for the shape. If the distribution conforms with a normal distribution, then the upper tolerance limit is determined by parametric statistics. If the distribution does not conform to normality, then, the theory of order statistics provide the tolerance limits and the associated confidence level. A more descriptive characterization of this approach being *a posteriori* would be the fact that there is no *a priori* conclusion on what the distribution should look like, consistent with many applications of statistics. This approach is completely in-line with the regulatory guidance provided in RG 1.157 that states:

> "*If a normal distribution is selected and justified, the probability limit can be conservatively calculated using two standard deviations. The added conservatism of the two standard deviations compared to the 95th percentile is used to account for uncertainty in the probability distribution.*"

TRACG methodology uses 2.024 times the standard deviation to account for uncertainty in the probability distribution due to number of sample calculations.

LTR Impact

GEH will reword LTR changing multiple references of "95/95" to read "95th percentile with high probability".